WEATHER AND SEASONAL CLIMATE PREDICTION OF ASIAN SUMMER MONSOON

T.N. KRISHNAMURTI1

Department of Meteorology, the Florida State University
Tallahassee, Fl 32306-4520, USA
E-mail: tnk@io.met.fsu.edu

Abstract

This paper provides a review for some aspects of numerical weather prediction of the monsoon. Here the data issues, state of monsoon forecasts of the current major global models, some results from regional high-resolution models, the area of cumulus parameterization, and how perhaps we might cope with its difficulties are addressed. The major issues of organization of convection and how high-resolution models are addressing those is also being discussed here. The promise of the multimodel ensembles and the superensemble for improving the state of forecasting of the monsoon is described in this paper. These procedures provide insights on performance of various cumulus parameterization schemes as well. A short review on month long forecasts of the low frequency motions such as the Madden-Julian Oscillations (MJO) and the Intra-Seasonal Oscillations (ISO) of the monsoon are included in this paper. Finally a summary is provided on possible areas of future work that emphasizes the need for more detailed observations over regions of steep orography and heavy rains; and the modeling issues related to these regions.

1. Introduction

A short review of the current state of monsoon forecasts over Asia are presented here. Monsoon forecasts span from the time scales of a few days to a season. Here the emphasis is on Numerical Weather Prediction (NWP) methods. Numerous groups in USA, Japan, Australia, China, Europe, and India have made major contributions in this area of research and operational practice. In this review on numerical weather prediction of the monsoon, we show the current performance of several numerical models. In recent years, major advances have occurred in data quality (those from surface, aircraft and space based), assimilation, modeling in terms of resolution, representation of orography, physical parameterizations of shallow and deep convection, radiative transfer (treatments of clouds, details of diurnal changes and surface energy balance), surface and planetary boundary layer physics for the fluxes of heat, moisture and momentum, and the inclusion of land surface processes. Both high-resolution global, and very high-resolution regional non-hydrostatic microphysical models have been deployed by numerous scientists to address the issues of monsoon life cycle. Forecast skills have been gradually improving during the last two decades. Monsoon precipitation is one of the central scientific issues. Improvements in forecasting daily rainfall on the medium range time frame of 5 to 7 days have come about from the use of improved physical initialization and the ensemble forecast approaches. In this review we shall provide a short account on monsoon forecasts from this perspective.

Physical initialization is a means for the improvement of the nowcasting of rain. This has been formulated for different models that use different cumulus parameterization schemes, Krishnamurti *et al.*, (1991), Treadon (1996). It has been possible to improve the nowcasting skill of precipitation that provides a correlation between the modeled initial rain and the satellite-based estimates to around 0.9 in a very consistent manner. That has been shown to have a major impact on the short-range forecasts

[1] Corresponding Author: T.N. Krishnamurti, Department of Meteorology, Florida State University, Tallahassee, Fl 32306-4520 USA, Tel: 850 644 2210, Fax: 850 644 9642, E-mail: tnk@io.met.fsu.edu

of the monsoon. Studies on models' sensitivity to other physical parameterizations have been somewhat limited.

In the context of the multimodel ensemble and superensemble forecasts (Krishnamurti *et al.*, 1999, 2000a, 2000b, 2001, 2002), we show the current performance of a number of lead models over the monsoon domain. We present here the skill scores for medium range forecasts of winds, sea level pressure and precipitation. These were all part of a real time global forecast model intercomparison. We note here that a measurable improvement in skill between 10 to 30 percent is achievable, compared to all member models, from the construction of a multimodel superensemble.

Finally we show some results on forecasts of the Intra-Seasonal Oscillations (ISO) of the monsoon that are carried out using a frequency filter within a low-resolution global model (Krishnamurti *et al.*, 1982, 1990c, 1992). That filter is only deployed at the initial state to remove all high frequency motions, the initial state thus includes only a time mean state and a low frequency, and the SST anomalies are prescribed. We show that the prediction of one cycle of the low frequency has some skill. That information can be used to provide some guidance for the occurrence of the wet and dry spells of the monsoon roughly a month in advance.

2. Weather and Climate Modeling of the Monsoon using Regional Models

a. Limited Area Models

With increasing economic activity, demand for high-resolution mesoscale meteorological information if growing rapidly for the monsoon region. For a number of regions of the world, regional mesoscale models at high-resolution have shown that they can provide realistic short-range forecasts. Developed nations have put huge resources for real-time regional NWP. With availability of enhanced computing and communication resources, efforts on regional numerical prediction for monsoon also have increased in Asia. At India meteorological Department (IMD), New Delhi, the Florida State University Limited Area Model (FSULAM) (Krishnamurti *et al.*, 1990b) has been run operationally for short-range weather prediction and for tropical storm prediction over the monsoon region. A host of community based regional mesoscale models is available freely for research and real-time use. As the requirement of high resolution (horizontal and vertical) increasing, the need for non-hydrostatic computations is becoming common. However, the requirements for mesoscale predictions over the complex mountain regions of the Himalayas are different (Das *et al.*, 2003).

Numerical modeling for the tropical low-latitudes and especially for the Asian monsoon was initiated at the Florida State University about 3-4 decades ago. Those studies were carried out with the FSULAM at various horizontal and vertical resolutions, having detailed computations for the physical processes (Krishnamurti, 1969, 1987a, Krishnamurti *et al.*, 1990b). The semi-lagrangian advection scheme coupled with semi-implicit time integration scheme for the tropical weather systems were appropriate and computationally economical. Use of generalized normal mode initialization for high-resolution (50 km) tropical monsoon modeling was introduced for FSULAM. This state-of-the-art limited area model could simulate the movement/landfall of tropical storms and was capable of predicting monsoon rainfall events. However, during those initial years, lack of proper observational data and assimilation schemes to produce mesoscale analyses were major hurdles for more accurate prediction of monsoon systems. The model prediction skill is quite sensitive to initial and boundary conditions. With the availability of unique high quality data sets (FGGE/MONEX, AMEX), the FSULAM was capable of predicting the genesis and track movement of monsoon disturbances. The importance of soil-moisture and associated feedback was realized for monsoon prediction using FSULAM (Dastoor and Krishnamurti, 1991).

The FSULAM at the IMD is being used on daily basis for the Indian Monsoon region for the last two decades. It consists of 1o lat/lon horizontal resolution with 12 vertical sigma levels. The boundary conditions and the initial analysis are taken from the operational version of NCMRWF global spectral model. The flow field and precipitation from real time short-range forecasts associated with the summer and winter monsoon for the Indian region is represented well by the this limited area model (Roy Bhowmik and Prasad, 2001). However, as expected, at this low resolution, the orographic rainfall associated with the Western Ghat Mountains of India is under predicted. During post-monsoon period, when the orographic rain decreases and the rainfall belt moves to peninsular India, the skill of this model is found to be much higher. By prescribing realistic initial moisture field (from INSAT IR data) over the Bay of Bengal and Arabian Seas, the skill of the precipitation forecast associated with movements of monsoon depression was improved considerably (Rao *et al.*, 2001). When the model resolution is enhanced to 50 km and 16 vertical levels, it could capture the mesoscale convective organization associated with cyclonic storm and monsoon depression more realistically (Roy Bhowmik, 2003). With enhanced resolution, the model could capture the heavy rainfall belt along the Western Ghats as well.

A version of NCEP's mesoscale ETA model is being used operationally at NCMRWF, India for the monsoon region (Rajagopal and Iyengar, 2002) for producing forecasts up to 3 days. The horizontal resolution is 32 km, and in the vertical, it has 38 layers. The mean layer depth in PBL is roughly 20 meters. The initial and the boundary conditions are interpolated from the NCMRWF global spectral model analysis and forecasts. The initial soil moisture and soil temperatures (3 layers) are taken from the same global model. However, real-time SST, snow depth and snow cover analyzed by NOAA/NCEP is used in real time as other surface boundary conditions. It produced more details of rainfall distribution and intensity associated with the west coast and the Himalayan orography.

b. Nested Regional Models

Nested regional models for the monsoon are useful for providing regional details both in weather and climate predictions. Kanamitsu and Juang (1994) simulated the Indian monsoon by nesting the NCEP regional spectral model (~ 40 km/18L) to the NCEP global spectral model (T62/18L). The onset and progress of monsoon for the year 1992 and the associated rainfall distribution was more realistic in the regional nested model simulation. In another study, the NCEP ETA model (80km/38L resolution) was nested to spectral COLA GCM (R40 / L18) to simulate the contrasting 1987/1988 monsoons. The nested high resolution ETA model could simulate the anomalous distribution of rain in a more realistic way (Ji and Vernekar, 1994).

c. Very High Resolution Mesoscale Regional Models

The fifth generation PSU/NCAR non-hydrostatic Mesoscale Model (MM5) has been installed and tested for real time application for the Indian monsoon domain since 2002 (Das, 2002). The model has been tested for the region with triple nesting at 90 km (Asia), 30 (India) and 10 km resolutions. The innermost domain of 10 km has been placed over the different orographic regions and regions of special interest to predict the mountain and severe weather patterns. The model was also tested at cloud resolving scale (1 km resolution) for a heavy rainfall episode. Several weather systems during active monsoon conditions, heavy rainfall events, tropical cyclone and western disturbances have been simulated by the model with interpolated initial conditions taken from the NCMRWF/NCEP T80 global model analysis produced at NCMRWF operationally. At present, a variational data assimilation system developed for MM5 at NCAR (Barker *et al.*, 2004) is being adopted at NCMRWF for operational use to produce mesoscale regional analysis. Mesoscale analysis from this system will help in evaluating the model skill for the monsoon systems.

A version of ARPS model of CAPS/OSU was also used to simulate two cases of monsoon systems (Vaidya *et al.*, 2004) at two different resolutions of 50 km and 25 km grid spacing with 25 vertical levels. The GEWEX 1.25° Lat/Lon resolution analysis was used for the initial and boundary conditions. The details of the flow fields and precipitation associated with the features of the sub synoptic patterns are verified reasonably with the observed analysis.

3. Monsoon Forecasts using Global Models

a. Sensitivity to Global Model Resolution

We shall next provide a summary of monsoon modeling related to the resolution issue. Krishnamurti (1990a) carried out forecasts at various resolutions of a global model (Triangular truncation T21, T31, T42, T63, T106 and T170), these range in resolutions of transform grid spacing between 6 degrees to roughly 0.7° Lat/Lon. In this example the location of a monsoon depression at day 5 of forecast was examined. It was noted that as the resolution increased, the location was slowly placed by the forecasts very closed to the observed location of the depression. This is illustrated in Fig. 1, where the observed flow field on day 5 at the 850 hPa is used as a reference, and dark points indicate the locations of the centers of circulation for the various experiments with different horizontal resolutions. Since organized convection is a very important process for the evolution of the monsoon, it is not surprising that increased resolution would improve these forecasts. In a later study, that resolution was increased by Krishnamurti *et al.*, (1998a) to T255 (which has a transform grid separation of around 45 km). In these experiments, improved monsoon circulation forecasts included distribution of organized convection of mesoscale precipitating rain elements that resembled closely to the observed precipitation signatures, these are illustrated in Fig. 2(a, b). In this context, it should be noted that it is not imperative that one needs a mesoscale non-hydrostatic microphysical model for the accurate forecasts of the large scale monsoon, it is the ability of the model to predict the organization of mesoscale precipitating clusters that is more important. The dimensions of the meso scale precipitating clusters are of the order of 300 km, and at a global resolution of T255, those are resolved by at least 8 transform grid points, thus a good cumulus parameterization scheme within a high-resolution global model can carry and predict their organization as was seen in this study. Predicting accurately each and every cloud may be important for defining the detailed structure of the mesoscale cluster, but a high-resolution global model can effectively predict the organization of convection out to at least 3 days.

b. Month Long Forecasts of Monsoonal Intra-Seasonal Oscillations

Other promising parallel efforts on the prediction of dry and wet spells of the monsoon have emerged from statistical rather than deterministic efforts by many authors. In a recent study, Goswami and Xavier (2003) noted from an analysis of historical data sets that there is a possible potential predictability exits through almost 20 days in advance for break periods of the monsoon. The potential predictability of active spells is only of the order of 10 days. The former appears to have large-scale controls (Krishnan and Kasture, 1996), whereas the latter seem to have thermodynamic control as well.

In a series of papers, Krishnamurti *et al.*, (1982, 1990c, 1992), addressed a methodology for predicting the monsoonal Intra-Seasonal Oscillations (ISO) on the time scale of 30-50 days. Because of the relationships of the ISO to the dry and wet spells of the monsoon, this topic is of considerable practical interest. This series of papers addressed forecasts over India, China and Australia. The methodology consists of prescribing an initial state for an atmospheric global model, Krishnamurti *et al.* (1998b), as the resolution T21 (21 waves Triangular Truncation). That initial state is derived from roughly 120 days of past data sets. A band pass filter is deployed to extract the ISO time scale

anomalies i.e. perturbation on the time scale of 30 to 50 days. Let us call it Q_{ISO}. There is also a 120-day average value $\overline{Q}$ that denotes a recent time mean of that variable. The initial state for any variable Q is simply $\overline{Q} + Q_{ISO}$ and this essentially filters out all high frequency motions. The sea surface temperatures are similarly extracted to define the initial values. Since this is an atmospheric model, the future oceanic state of the SSTs are simply obtained from an extrapolation of the SST anomalies from the past 120 days into the future. Here the future projection is done by extrapolation of the phase and amplitudes of the harmonic wave time series of the SSTA at each grid point. This permits the slight movement of the SST anomaly over a one-month period while the range of forecast being studied here.

This models initial state was so designed because the highest frequency modes have predictability for a period of only one week. There are some very strong interactions between the ISO time scale motion and the high frequency motions. Thus, the errors in the latter, after a one-week integration, lead to large errors for the ISO. Filtering out these higher frequencies initially suppressed growth of such errors at least through one cycle of the dry and wet spell, and it was thus possible to push the forecasts of the ISO to well past one month. Even in these experiments where the higher frequencies are initially absent, they still grow after a few cycles; see Fig. 3. Here results of integration over several cycles and a rapid growth of the higher frequencies are clearly apparent after a few cycles of the ISO time scale. In these integrations we noted a marked predictability for the ISO on a one-month time scale, thus making it possible to address the issues of monsoonal dry and wet spells.

Figure 4 illustrates the ISO based on observations and the model forecasting for days 5, 10, 15, 20, 25, and 30. These are the wind fields at the 800-hPa levels on the time scale of the ISO. In this example the analyzed (observed) and the model predicted fields show a great degree of similarity during an entire one month forecast. The cyclonic and anticyclonic lobes of the low frequency motion move meridionally and the predictability for the ISO appears quite high. The dry and wet spells of the monsoon relate to the presence of parallel and antiparallel flows. If these predicted anomalies are parallel to the climatological monsoon circulations, they tend to enhance the monsoon and a wet spell prevails. Generally, the antiparallel geometry favors a dry spell. In that sense this one-month forecast was very successful in predicting the intra seasonal wet and dry spells during the first month of this forecast. It is also possible to assess this skill quantitatively. For this purpose, an anomaly correlation of these forecasts was estimated from the 850 hPa streamfunction and is shown in Fig. 5. The anomalies over the global domain (Fig. 5a) and for the tropical region (Fig. 5b) were predicted here at an anomaly correlation of 0.6. This is a reasonably high value for the forecast of an anomaly. Thus, overall this appears to be a promising method for predicting the passage over a month long period for the ISO anomalies.

One obvious limitation of this model is the initial loss of skill in the first five days. That is clearly apparent in Fig. 3. That loss of skill is attributed to a lack of proper initialization of the low frequency initial state. The low frequencies were extracted from past data for all variables but no effort was made to establish any kind of a balance for the different variables. Relating first the low frequencies and assuring a balance among variables is not a trivial task. That area requires further research, if that were possible we may be able to prevent the initial loss of skill and produce even better forecasts than one displayed here.

4. Monsoon Forecasts and Sensitivity to Physical Parameterization Schemes

A number of recent studies have addressed the issues of physical parameterization to the modeling of the monsoon. Among the different areas, that of cumulus parameterization has drawn the most interest, Eitzen and Randall, 1999, Alapaty *et al.*, 1994, Slingo *et al.*, 1994, Zhang 1994, Rajendran *et al.*, 2002 etc. Alapaty *et al.*, (1994) used the NRL/NCSU regional nested model (Madala *et al.*, 1987)

to study the impact of two different convection schemes (Kuo and Betts-Miller) on the prediction of the winds and precipitation for one case of monsoon depression. In this experiment, the finer resolution grid was 0.5° Lat/Lon and was nested to a coarser 1.5° Lat/Lon grid. Their conclusion was that the Kuo scheme performed better for that case. Inclusion of parameterization for the land surface processes made the simulations better in a case study (Raman *et al.*, 1998). In another case study, using the same model in a triple nested set up the importance of orography in the west coast was shown for the heavy rainfall events (Wu *et al.*, 1999). Cumulus parameterization is still somewhat adhoc and does not blend with a large-scale model in a very natural way, i.e., the dynamics and physics are somewhat unconnected in the sense that they are different components of separate computations that are carried out sequentially within the time step of a model. It is however quite apparent that monsoon evolutions in prediction models are very sensitive to the particular cumulus parameterization one deploys. A cumulus parameterization scheme within a certain model behaves somewhat differently if the same scheme is used in a different model. This has to do with the fact that model resolutions, formulations of dynamics, rest of the physics, the boundary conditions and the treatment of orography all end up dictating how a particular scheme equilibrates with that cumulus parameterization scheme within one model. Thus it is somewhat meaningless to state that scheme A is superior to scheme B from tests performed with a single model. However there are some gross distinctions on the formulations of different schemes that do spell out the superiority of one scheme over another regardless of what diverse models they are tested with. For example, a hard convective adjustment does not properly represent the effects of an ensemble of clouds. Some schemes do not describe the vertical structure of heating or moistening very well. Such deficiencies can be explored using semi-prognostic tests using well-established field experimental data sets such as those from GATE or TOGA-COARE.

For the monsoon systems, a number of case studies have been undertaken to study the impact of parameterization procedures available for different physical processes. Unfortunately, the results are heavily dependent on model formulation, model resolution and the weather system itself. Any particular model at a fixed resolution behaves in a particular way for one type of weather systems. Each tropical monsoon weather system is unique in its structure, evolution and interactions. It becomes very difficult to conclude the impact of parameterization of physical processes on precipitation forecasts. Observed data from field campaigns (MONTBLEX, INDOEX, BOBMEX, ARMEX) will be perhaps useful to understand the physical processes associated with different monsoon weather systems. Then depending on the scale of interest, a particular set of parameterization algorithms can perhaps be combined for optimum performance for a model. In this section, various physical parameterization schemes and their impact on monsoon related studies is reviewed.

a. Land Surface Processes

Demand for more realistic treatment of the processes at the land surface, in the vegetation and the soil, have led to the development of increasingly elaborate and explicit schemes. The most rudimentary treatments employ a prescribed moisture function for the calculation of the evaporation rate as a fraction of the potential evaporation. Such models have obvious shortcomings, especially for long-term integrations, since they do not respond to rain or drought in the course of the integration, and therefore evaporation feedback is lost. A step up from those is bucket models, first introduced by Manabe (1969), linking the ground wetness to the past rainfall through a simple empirical relationship. Such models do not explicitly model what happens in the soil below or in the vegetation above the surface.

A number of sophisticated land-surface schemes have been developed in the recent decade. The best known of those are BATS (Biosphere-Atmosphere Transfer Scheme) of Dickinson *et al.*, (1986)

and SiB (Simple Biosphere) of Sellers *et al.*, (1986), later succeeded by a simplified version, SSiB (Xue *et al.*, 1991). A number of similar land surface schemes have been developed recently, such as ISBA (Mahfouf *et al.*, 1995) and SECHIBA (Ducoudre *et al.*, 1993). All these models calculate the fluxes from the soil and canopy using similar principles with somewhat different formulation. Most have several soil layers and one or two vegetation layers; some use mosaic approach in which several types of vegetation are assigned fractional coverage of a grid box. A comprehensive summary of the different land-surface schemes used in the scientific community can be found in Henderson-Sellers (1993) and the issues associated with them in Garratt (1993). Off-line experimental results can be verified against surface observational measurements, such as those acquired during field experiments like HAPEX-MOBILHY (Andre *et al.*, 1986; Mahfouf *et al.*, 1996) and BOREAS (Sellers *et al.*, 1995). An intercomparison project - PILPS (Project for Intercomparison of Land Surface Parameterization Schemes) (Henderson-Sellers 1993, 1995) has been undertaken to evaluate the relative performances of a wide spectrum of LSS. Due to the limited amount of in-situ observations (and the difference in the GCMs into which the different LSS are introduced) it has proved impossible to name one superior scheme. It has been noted that the introduction of complex LSS has resulted in a significant disagreement between the different models, even if their underlying physical concepts are similar (Mahfouf *et al.*, 1996; Gates *et al.*, 1996). These differences (in the surface fluxes, and in the energy and hydrology balances) are present both in off-line experiments and in GCM simulations (Henderson-Sellers, 1995). The performance of the LSS depends heavily on the atmospheric models they are introduced into (Garratt, 1993). The partitioning of the incoming radiation at the surface into fluxes of sensible and latent heat and absorbed and emitted radiation is highly dependent on the properties of the land surface and its vegetation cover. Despite the significant progress in the development of detailed parameterizations of land surface processes over the last few decades, the relative importance of the degree of sophistication of the land surface treatment remains an open question in forecasts at seasonal time scales.

In the context of monsoon forecasts, this aspect of modeling is clearly more important for climatic time scales of a season or longer. However, since the land surface parameterization impacts the diurnal change a lot, it is worthy of examining this in the context of medium range weather prediction as well. A semi arid pre monsoon region has very large diurnal change in its surface physics, soon after the onset of monsoon that region becomes greener and has a much smaller amplitude for the diurnal changes. Modeling of such differences are important.

b. Various PBL Schemes Used for Monsoon Forecasts

The mixing of heat, moisture, momentum, and passive scalars is brought about by turbulence in the atmospheric boundary layer. In numerical models, the large-scale atmospheric flow determines to a large extent the properties of the PBL, and the PBL in turn reacts to these external forcings and modifies the large-scale flow. In order to explicitly resolve the boundary layer structure, several computational levels in the PBL of the numerical model are introduced. The formulations require turbulent terms of heat, momentum, and moisture at all these levels. Thus, in order to approximate or parameterize these turbulence terms, some kind of closure assumption is necessary to relate turbulent fluxes to mean quantities. Such closure assumptions can be classified by their statistical order and the degree of non-locality. While no parameterization is perfectly accurate, they offer a range of physical details and computation economies from which to choose. Basic closure schemes for all practical purposes are presently limited to the first, 1.5, second and third order. Second and third order closure schemes involve more physics of the boundary layer through increased formulation and numerical complexity. By and large, the closure assumptions used in numerical models are confined up to 1.5 orders.

Some of the PBL schemes being used currently are briefly described below.

The simplest way to close the system of equations is through first order closure in which the turbulent fluxes are related to the mean vertical gradients by an eddy viscosity coefficient K, which is a property of the turbulent flow. It is the eddy viscosity coefficient that must account for the complexities of turbulence. The problem of first-order closure is then effectively reduced to the problem of resolving K. Thus, for turbulent heat flux

$$\overline{w'\theta'} = -K\left[\frac{\partial \overline{\theta}}{\partial z}\right] \qquad (1)$$

The simplest and oldest approach to first-order closure is to specify K profile in which K is a constant. These constant K models are easily solved analytically but physically they are not well representative of the boundary layer because of their too simplistic approach. A more physically realistic approach is to prescribe a K profile that varies with height, thermal stability, local temperature gradient etc. Many authors including O'Brien (1970), Brost and Wyngaard (1978) have considered this approach to study a variety of atmospheric conditions.

All of these schemes are relatively simple and require only routinely measured or model resolvable meteorological variables to explicitly determine K. Thus K profiles are determined through parameters like $\frac{\partial \theta}{\partial z}, \frac{z}{L}, \frac{z}{h}$, where *h* is the PBL depth and *L* is the Monin-Obukhov Length. There is a drawback for these since the parameters are often not good indicators of the total turbulent flow.

Determining *K* empirically or through other meteorological variables has its own problems. A slight modification of this approach, known as mixing length approach in which *K* is expressed in terms of mixing length *l* such that

$$K_m = l^2\left[\left(\frac{\partial U}{\partial z}\right)^2 + \left(\frac{\partial V}{\partial Z}\right)^2\right]^{1/2} \qquad (2)$$

One must determine *l* instead of *K*. Prandtl (1932) had originally introduced the concept of mixing length in terms of atmospheric turbulence. He argued that the eddies that are responsible for carrying the parcel of air moves through a distance *l* known as the mixing length before adjusting the heat and momentum of the air parcel it is carrying with the surrounding air. Blackadar (1962) extended this hypothesis and reasoned that *l* varied as kz close to the ground (k being von Karman's constant) but approached some constant value λ at greater heights. Hence,

$$l = kz/(1 + kz/\lambda) \qquad (3)$$

Blackadar suggested equal to 2.7x10-4|G|/|f| where G is the geostrophic wind and f is the Coriolis parameter.

Based on a more detailed work of Louis (1979), the FSU global spectral model utilizes a local-*K* PBL scheme, in which *K* is not only dependent on *l* but also includes thermal stability functions that are dependent on a gradient Richardson number (*Ri*). Following Manobianco (1988) *K* is determined as,

$$K = l^2\left[\left(\frac{\partial U}{\partial z}\right)^2 + \left(\frac{\partial V}{\partial Z}\right)^2\right]^{1/2} F\left(R_i\right) \qquad (4)$$

where *l* is computed using (6) with λ set to 150m for momentum and 450m for heat and moisture. The stability functions, *F(Ri)* is of the form

$$F = \frac{1}{(1+5R_i)^2}, \text{ for stable conditions } (Ri \geq 0) \quad (5)$$

$$F = \frac{1+\alpha |R_i|^{1/2} - 8R_i}{1+\alpha |R_i|^{1/2}}, \text{ for unstable conditions } (Ri < 0) \quad (6)$$

with α taken 1.746 for momentum and 1.286 for heat and moisture. The gradient Richardson number for a given atmospheric layer is expressed as $R_i = \frac{\frac{g}{\theta}\frac{\partial \bar{\theta}}{\partial z}}{\left|\frac{\partial \vec{V}}{\partial z}\right|^2}$.

The operational version of the NCMRWF global spectral model that was running till July 2000 used a local-*K* PBL scheme with *K* determined through mixing length considerations as discussed above, but with semi empirical stability dependent functions based on a bulk Richardson number, *Rib* (Kanamitsu 1989, Basu *et al.*, 2002). The stability functions, *F(Rib)* is of the form

$$F = \frac{1}{(1+5R_{ib})^2}, \text{ for stable conditions } (Ri \geq 0) \quad (7)$$

and for unstable conditions (*Ri* < 0)

$$F = \frac{1+\frac{8}{\sqrt{21}}\sqrt{|R_{ib}|}+8|R_{ib}|}{1+\frac{8}{\sqrt{21}}\sqrt{|R_{ib}|}}, \text{ for momentum} \quad (8)$$

and,

$$F = \frac{1+\frac{12}{\sqrt{87}}\sqrt{|R_{ib}|}+12|R_{ib}|}{1+\frac{12}{\sqrt{87}}\sqrt{|R_{ib}|}}, \text{ for heat and moisture.} \quad (9)$$

There are certain basic limitations of the mixing length theory (Stull 1988) involved with the local-*K* approach. The most important drawback is its inability to realistically represent mixing in the convective boundary layer involving the "counter gradient fluxes" since the influence of large eddy transports are not accounted for (Holtslag and Moeng 1991). This affects the profiles of mean quantities especially in locations where dry convection is of importance in the PBL. One of the possibilities to overcome this problem is to utilize higher order closure approaches, which are computationally more expensive.

In the modified gradient approach or ***non-local*** corrected, the fluxes are still allowed to flow down the local gradient, but an artificial gradient g is added to the gradient during convective conditions (Holtslag and Moeng 1991). Thus

$$\overline{w'\theta'} = \text{-K } [\frac{\partial \bar{\theta}}{\partial z} - \gamma] \quad (10)$$

Here, g reflects the nonlocal transports due to dry convection.

Troen and Mahrt (1986) proposed a non-local *K* closure utilizing *K* profiles based on O'Brien (1970), in which the eddy diffusivity for momentum, *Km* was given as,

$$K_m = k\, w_m\, z \left(1 - \frac{z}{h}\right)^2 \qquad (11)$$

where *wm* is a mixed-layer velocity scale that depends on the surface friction velocity, the surface layer height (0.1h) and *L*. The eddy diffusivities for heat and moisture were derived using the Prandtl number relation *(Pr = Km/Kh)*. They used a simple diagnostic formulation for PBL height as

$$h = Rib_{cr} \frac{\theta_{va} \left| V(h)^2 \right|}{g\left(\theta_v(h) - \theta_s\right)} \qquad (12)$$

where *Ribcr* is the critical bulk Richardson number taken as 0.5 (Hong and Pan 1996), *V(h)* is the horizontal wind speed at *h*, θva is the virtual potential temperature at the lowest model level, θv(h) is the virtual temperature at *h*, and θs is the virtual potential temperature at the surface which is modified to include the influence of thermals for the unstable case.

It also incorporates the effects of nonlocal turbulent transports of heat and moisture by large eddies by parameterizing g in a simplified manner. Above the PBL, a local diffusion approach is applied with modified stability functions (see Hong and Pan 1996). This scheme has been widely tested in numerical models with suitable modifications (Holtslag and Boville 1993, Hong and Pan 1996 and others).

Basu *et al.*, (2002) compared the performance of a nonlocal closure PBL scheme following Hong and Pan (1996) with that of the local closure scheme (Kanamitsu 1989) in the NCMRWF global spectral model used for real time forecasts over the Indian region. Using a version of the NCMRWF model, Sanjay *et al.*, (2002) analyzed the temporal and spatial variability of simulated PBL height, based on Troen and Mahrt (1986), within the nonlocal scheme. A similar nonlocal *K* PBL scheme was introduced by Holtslag and Boville (1993) in the NCAR CCM2 model used for climate simulations. The formulation differs from that of Troen and Mahrt (1986) in the specification of surface turbulent scales and in the nonlocal turbulent effects.

An improvement to the simplicity of first-order closure could be achieved by introducing more of the physics of the atmosphere while accounting for the formulation of the eddy diffusivity coefficient keeping in mind the computational economy. Such a scheme is the Turbulent Kinetic Energy (TKE) closure where the K coefficient is determined by the TKE available in the atmosphere that is obtained prognostically. While Prandtl considered only mechanically induced turbulence, the TKE approach can also include the buoyantly generated turbulence and turbulence that is transported in from other locations. Within this approach, one needs a forecast equation for the TKE. Thus, knowing the TKE as well as the mean gradients, it is then possible to parameterize the fluxes. For turbulent kinetic energy E expressed as($\overline{u'^2} + \overline{v'^2} + \overline{w'^2}$)/2, the prognostic equation for TKE over a horizontally homogeneous surface can be written as follows:

$$\frac{\partial E}{\partial t} = -\overline{uw}\frac{\partial U}{\partial z} - \overline{vw}\frac{\partial V}{\partial z} + \frac{g}{\theta}\overline{w\theta} - \frac{\partial}{\partial z}\left(\overline{wE} + \frac{\overline{pw}}{\rho}\right) - \varepsilon \qquad (13)$$

where the first two terms on the right hand side represent shear production, the third term represents buoyancy production, the fourth turbulent transport and the fifth dissipation of turbulent energy. In this closure, several terms on the r.h.s. need to be parameterized. The TKE schemes are further classified into three schemes based on the prognostic variables considered. The first TKE parameterization considered is the "*l* model" where the mixing length *l* is modeled either diagnostically or prognostically. The diffusivity is determined through the mixing length and the turbulent kinetic energy available. The second is the "E-ε model" in which a prognostic equation for ε is developed. The diffusivity in this case is determined through the available kinetic energy and the dissipation. The final approach is known as the "E-*l* model" in which a prognostic equation for the

product E. *l* is used and the diffusivity is determined through the mixing length and available turbulent kinetic energy.

Incorporation of a "E-ε" TKE parameterization in the NCMRWF model (Basu *et al.*, 1998) showed a positive impact on the prediction of some important synoptic features over the Indian region, including the genesis of monsoon lows, better tracks of monsoon depression, and on precipitation forecasts.

Second and third order closure carries forecast equations for not only all the mean variables but also for all the second order and third order terms respectively. Some also include forecast equations for dissipation rate. Third and higher order correlations and pressure correlation terms must be parameterized. Most of these parameterizations utilize down-gradient local diffusion. The scope of including one such higher order PBL scheme for this work is also important for monsoon studies.

c. Sensitivity of Monsoon Forecasts to Cumulus Parameterization

An interesting example on the sensitivity of monsoon forecasts to cumulus parameterization was illustrated by Krishnamurti *et al.*, (1987b). Here two versions of the so-called Kuo's scheme were used to examine the onset of monsoon for the year 1979. That year the onset was preceded by the formation of a tropical cyclone (called the onset vortex) in the Arabian Sea, thus the prediction required forecasting the formation and motion of this tropical cyclone and the development of a strong moist current to its south as the monsoon over India got established. That was a medium range forecast experiment using the FGGE data sets. Figure 6 (a, b, and c) illustrate the 850 hPa level winds at the initial time and those at hour 144 for the two versions of the cumulus parameterization schemes, and also shown are the day 5 observed fields (Fig. 6a). It is apparent that one version of the Kuo's scheme, called a classical Kuo's scheme, Kuo (1965), failed in this monsoon simulation while a second one that was a modified scheme, (Krishnamurti *et al.*, 1983) provided a very promising simulation. The former scheme was noted to provide strong moistening and was deficient in its definition of heating and rainfall rates. The latter scheme had been statistically improved to reduce that deficiency. The message here was clearly that monsoon simulations were strongly affected by the cumulus parameterization scheme one deploys.

In a recent paper Krishnamurti and Sanjay (2003) addressed the impacts of six different cumulus parameterization schemes (see Table 1 for a description of these schemes) in a large number of numerical forecast experiments. All of these experiments utilized the same model, the FSU global spectral model, described in Appendix 1. All these runs utilized the same initial states, a total of some 120 experiments were carried out from each of the 6 models. This provided a large sample of experiments to investigate the behavior of the different cumulus parameterization schemes. These were all one-to-two-day long integrations. Since the only differences were in the cumulus parameterization, the premise here was that the differences that arise in a one or at most two-day forecasts might largely reflect the behavior of the cumulus parameterization schemes, since all other factors were the same in the different models. The most important variable for these tests was the predicted rainfall. Skills such as the rms errors and anomaly correlations were evaluated for this large number of experiments to assess the performance of the different schemes. We also constructed a multimodel ensemble mean forecast and a superensemble (discussed in section 5 of this paper) from these same data sets of day 1 and day 2 of forecasts. In addition to these we also designed a synthetic cumulus parameterization scheme (named as the Unified Scheme) that included within one single model the weighted sums of all of the six cumulus parameterization schemes. Those weights were simply borrowed from the day one forecast weights of the multi model superensemble. Since the six cumulus parameterizations are based on different physically based features, the unified scheme carries all of these features in a weighted sense. Details of this construction of this scheme are provided in Krishnamurti and Sanjay (2003). Figure 7 illustrates the forecast skills of one and two-day forecasts

of precipitation from the member models, from the ensemble mean of these models, those from the unified model and those from the multimodel superensemble. It is clear from this large volume of experiments that the performance of different cumulus parameterization schemes is not drastically different from each other. One of these schemes, i.e., the relaxed Arakawa Schubert scheme did seem to perform slightly better than most other schemes. However, when we examined the day-to-day performance, we did find that the daily skill curves of these member models did intersect often, implying that a superior or inferior performance on a given day by a certain scheme did show an initial state dependence. The unified model did perform better than each of the member models, implying that a collection of physically based processes that call for cumulus convection is better than the use of single scheme that do not include all possible processes. What surprises here is the result from the multi model superensemble; that stands out far superior to all others shown here. That is not surprising since that does include a training phase where the collective bias errors of the member models are corrected in the construction of the superensemble forecast (see Section 5).

d. Organization of Convection and Monsoon Forecasts

The organization of monsoon convection is an important model simulation problem. It has been shown that one needs almost a mesoscale resolution over the globe to simulate these features. We had noted that if we perform physical initialization of precipitation at a very high global resolution, such as T255 (which has a transform grid separation of roughly 45 km), it is possible to fully retain the organization of convection described by mesoconvective precipitating elements (scale of the order of 300 km). Furthermore, we find that such an organization of convection is in fact carried into the future in medium range forecasts by this high-resolution model. This is an important issue for various scientific reasons. Gill (1980) provided a fundamental rationale for associating tropical motions to the distribution of heat sources and sinks. In the tropics, that relationship is very strong, the monsoon being an excellent example. These so called heating forced solutions were extended over the entire global tropics by Zhang and Krishnamurti (1996). There it was shown that the climatological flows of the lower troposphere for the summer monsoon could be obtained as exact solution from prescribed heating using parabolic cylinder functions and trigonometric functions as basis functions within a linearized shallow water framework. The lower tropospheric monsoon circulation of the Asian summer monsoon is described by an inverted "letter S". That inverted S starts from the southern trades, then on to the cross equatorial flows across the equator along the Kenya-Somalia coast, and then follows the southwest monsoon flows and terminating in a monsoon low south of the Himalayas. Along this inverted S a steady growth of convection can be seen with the heaviest convection in the foothills of the Himalayas. Along the inverted S an organization of convection can be seen paralleling these low level flows. We believe that this organization of convection is central to the maintenance of a robust monsoon. Thus the modeling of this organization is very important. It turns out that, with a parameterized cumulus convection, instead of explicitly resolving each cloud and its organization, we can resolve the organization in medium range forecasts if the hydrostatic model has a sufficiently high resolution.

e. Radiative Interactions for the Monsoon Modeling

There are three well known schemes for the parameterization of radiative transfer that are used in most models for the prediction of the monsoon. These are the classical Emissivity/Absorptivity based model, Chang (1979), the Band model of Lacis and Hansen (1974), and explicit cloud models, Zhao (1997). The importance of radiative transfer for the modeling of monsoon became clearly evident from Yanai *et al.*, (1973) studied on the heat sources and sinks where they showed that the apparent heat source Q1 minus the apparent moisture sink Q2 is of the order of the radiative heating R. The vertical eddy flux of heat that is central for monsoon simulation is directly proportional to Q1-Q2-R,

thus an inclusion of the radiative forcing is important even for short to medium range prediction of the monsoon. Having said that, when one looks at the literature on this topic, we find that not many studies have been devoted to the issue of monsoon modeling sensitivity to radiative transfer. Further work is needed to address this problem considering the importance of differential heating of the monsoon that requires an accurate modeling of the radiative forcing over regions of the heat sinks. Another major monsoon issue is the modeling of the diurnal change that shows up in the surface fluxes and in the phase of convection and rainfall. Over a short distance of several hundred km from eastern Tibetan Plateau and the foothills of the Himalayas, the phase of the diurnal change varies from an afternoon convection to an early morning convection. These appear to be driven by cloud radiative and surface flux processes. A careful modeling of the phase of the diurnal change is important for the monsoon forecasts. The scales of the monsoonal diurnal change can be very large covering several thousand km, Kishtawal and Krishnamurti (2001), and on that scale a direct coupling of the diurnal cycle with the monsoon circulation seems to be apparent.

5. Multi Model Forecasts for Weather and Climate

One of the most powerful approaches for weather and seasonal climate forecasts utilizes a multimodel superensemble was described in Krishnamurti *et al.*, (1999, 2000a, 2000b, 2001, 2002, 2004). The superensemble methodology utilizes a vast collection of past forecasts by member models to assess their collective biases and to utilize that statistics towards the correction of forecasts into the future. Given some 10 such member models providing forecasts over an array of roughly 100,000 locations at ten vertical levels for 10 variables that statistics ends up including some 10 million correction weights. Examination of those weights show that most models have some areas of major skills, thus a superensemble is in some sense the collective wisdom of the multi models. We use somewhat different methods for obtaining this statistics for weather or the seasonal climate forecasts; these are briefly described in the next two sections.

a. Conventional Superensemble Methodology

The superensemble technique produces a single consensus forecast derived from a multimodel set of forecasts. Superensemble forecasts carry the highest skill compared to participating member models, their ensemble mean and the bias-removed ensemble mean representations. The methodology to construct the multimodel superensemble consists of partitioning the time line into two components – the training phase, and the forecast phase. During the training period, the multimodel forecasts and the benchmark observed (analysis) fields are utilized to derive model performance statistics, which are then passed on to the forecast phase where multimodel forecasts are weighted as per their past performance to obtain superensemble forecasts.

In the training phase it is possible to derive statistics on the past behavior of the multimodel with respect to the observed analysis. Using a multiple linear regression technique, in which the model forecasts were regressed against an observed (analysis) field through a least squares minimization of the difference between anomalies of the model and the analysis fields, distribution of weights is determined for each member model. These regression coefficients associated with each individual model conceivably can be interpreted as a measure of that model's relative reliability for the given point over the training period.

The definition of the conventional superensemble forecast is given by:

$$S = \overline{O} + \sum_{i=1}^{N} a_i \ (F_i - \overline{F}_i) \qquad (14)$$

where S is the superensemble prediction, $\overline{O}$ is the observed time mean (during the training phase), a_i are the weights for individual models *i*, F_i is the predicted value from model *i*, $\overline{F_i}$ is the time mean of prediction by model *i* for training period and N is number of models. The weights are computed at each of the transformed grid points by minimizing the objective function *G* using least square minimization of the error of the forecasts:

$$G = \sum_{t=0}^{t=train} (S_t - O_t)^2 \qquad (15)$$

where '*t*' denotes the length of a training period.

In this conventional superensemble methodology for weather and season climate forecasts, a sequence of individual forecasts from several models are collected and subjected to multiple linear regression against the observed (or assimilated) counterpart fields and the coefficients are stored for each of the member models. The length of the training data varies for each type of forecast. For medium range (1-6 days into the future) forecasts, about 120 days of training is found required while for seasonal climate forecasts about 10 years of multi model forecast data sets would be necessary. The weights collected during the training phase are passed on to the forecast phase of the superensemble. In the forecast phase, the member model forecasts are corrected collectively, using the regression weights. This type of local bias removal is more effective compared to a conventional bias removed ensemble mean where a weight of 1.0 is assigned to all models after bias removal. The superensemble procedure assigns fractional and even negative weights to the model forecasts depending on their past behaviors.

b. Synthetic Superensemble Methodology

In order to achieve higher skills for seasonal climate forecasts, a variant of the above conventional superensemble formulation was proposed by Yun *et al.*, (2004). In this procedure, additional "synthetic data sets" are constructed from the member model forecast data using a combination of the past observations and past forecasts. A consistent spatial pattern is determined among the observations and forecasts using a linear regression relationship in the EOF space. Sets of such synthetic forecasts are then obtained for each available member model forecast and used for the creation of superensemble forecasts. The synthetic data generation and the associated statistical procedure are described below.

The time series of any observation field *x* can be written as a linear combination of EOFs such as,

$$O\ (x,t)\ =\ \sum_{n}\ \ P_n\ (t)\ .\ \phi_n(x) \qquad (16)$$

where *n* is the number of modes selected. The two terms on the right hand side of above equation correspond to the time (principal component PC) and space (EOF) decomposition respectively. PC time series P(t) represents how EOFs (spatial patterns) evolve in time. These PCs are independent of each other. In a similar manner the forecast time series is projected into the PCs and EOFs for m member models,

$$F_i(x,T)\ =\ \sum_{n}\ \ F_{i,n}\ (T)\ .\ \varphi_{i,n}(x) \qquad (17)$$

Here index *i* represents a particular member model. Using a regression relationship between the observation PC time series and a number of PC time series of forecast data, it is possible to deduce the

spatial patterns of forecast data, which evolve in a consistent way with the EOFs of the observation for the time series considered. The regression relationship is given by

$$P(t) = \sum_n \alpha_{i,n} F_{i,n}(t) + \varepsilon(t) \quad (18)$$

Here the observation time series P(t) is expressed in terms of a linear combination of forecast time series F(t) in EOF space. The regression coefficients αn are found such that the residual error variance E (ε2) is minimum. Once the regression coefficients are determined, the PC time series of synthetic data can be written as:

$$F_i^{reg}(T) = \sum_n \alpha_{i,n} F_{i,n}(T) \quad (19)$$

Then the synthetic dataset is reconstructed with EOFs and PCs as:

$$F_i^{syn}(x,T) = \sum_n F_{i,n}^{reg}(T) \,.\, \phi_n(x) \quad (20)$$

These synthetic data (*m* sets) generated from *m* member model's forecasts are now subjected to conventional FSU superensemble technique (Krishnamurti *et al.*, 2000a) described in this section.

c. Performance of Multimodels for Weather and Seasonal Climate Forecasts

Here we shall illustrate some of the current skills of weather forecasts for the Asian summer monsoon. The domain here extends from 50°E to 110°E longitudes and 10°S to 35°N latitudes. These are typical real time forecast results for a year (this covers the skills for June, July and August 2001). We illustrate in Fig. 8 (a, b, c, d, e and f) the skills of forecasts through days 3 (for precipitation) and 5 (for winds and MSLP). Panel 'a' shows the bias of the equitable threat scores for precipitation forecasts for rainfall rates in excess of 5mm/day. The skill metrics are described in Appendix II. A bias score near 1.0 is a perfect score. There are 6 member models included here, these are in fact some of the major operation models that carry out monsoon forecasts on a daily basis, these include models from UK, USA, Japan, Australia and Canada. Bias errors of the various models range from 1.0 to 2.3. The dark barb shows that it is possible to consistently reduce the bias errors consistently to a value around 1.0 from the construction of the superensemble. Panels 'b' and 'c' show the precipitation forecast skills for thresholds of rain rates greater than 5 and 0.2 mm per day respectively. These are skills for days 1, 2 and 3 of forecasts. The superensemble skills clearly stand out over the monsoon region. For thresholds of precipitation rates above 0.2 mm/day the three-day skills of around 0.7 are indeed most impressive, considering that most member models have values generally below 0.5. For heavier rains, threshold greater than 5 mm/day the superensemble is still quite impressive with equitable threat values around 0.35 or above whereas the member models have values closer to 0.2. We also present the rms errors of precipitation forecasts of the member models and of the superensemble in panel 'd', where we can see a reduction of the error from the superensemble compared to each of the member models. Shown in panel 'e' are the rms errors of the vector wind at 850 hPa level. These are again slightly better for the superensemble compared to all the member models. The corresponding results for the rms errors for the sea level pressure are shown in panel 'f' where we note a major reduction of sea level pressure errors from the multimodel superensemble. Over all, in NWP of the monsoon this degree of improvement is generally possible for 3 to 5 days of forecast length from the deployment of the superensemble

The results on the seasonal forecasts for the Asian summer monsoon are described here. These results are based on 11 member models, and cover a total of some 15 years of data sets. The length of this data set is still not sufficiently long to separate the training period from the forecast phase distinctly, for this reason a cross validation technique is used here, that uses all forecasts in training phase successively, always excluding the particular season that is being forecasted. This enabled us to

obtain a reasonable data length for the training phase. When more and more years are included, this use of cross validation would not be necessary. Forecasts are made at the start day of each month and over all we have a total of some 17 seasonal forecasts on which the monsoon forecast skills are being prepared here, for details see Krishnamurti *et al.*, (2004). Tables 2 and 3 describe briefly the basic ingredients of the 11 models. Among the 11 models 7 belong to a European family called DEMETER, Palmer *et al.*, (2004). The remaining 4 models are variants of a single FSU model where different permutations of physical parameterizations are deployed in the otherwise same model. All eleven of these are coupled global atmosphere-ocean models. Coupled models are better suited for seasonal time scales since the temperature anomalies do change over the time scale of 3 to 4 months. Here we shall provide a summary on the performance of single models, their ensemble mean performance and that of the synthetic superensemble for the seasonal Asian summer monsoon rainfall. The results here are presented in terms of the standard skill scores (see Appendix II) such as the rms errors over the monsoon domain and the anomaly correlations. We shall also present comparative maps on the performance of models for a selected season for illustrative purposes.

In Fig. 9 (a and b) we present the seasonal forecast errors for each year of forecast for the Asian summer monsoon. Here Fig. 9a shows the results from the DEMETER models and Fig. 9b shows those from the FSU suite of models. Within each panel the top diagram carries the rms errors of the 7 member models, the results of the ensemble mean of the DEMETER member models, the ensemble mean for the synthetic models and finally the synthetic superensemble. We also show the anomaly correlations for the same within each panel. These are the seasonal forecast skills for precipitation over a domain covering the longitudes 50°E to 110°E and from 30°S to 30°N. The member model's rms errors in seasonal precipitation are around 2.6 mm/day and are reduced from the deployment of the synthetic superensemble to around 1.7 mm/day. The corresponding improvements for the anomaly correlations go from around 0.3 to 0.4 from the synthetic superensemble. The results for the FSU suite of models show somewhat greater degree of improvements compared to the DEMETER suite. Thus it is clear that monsoon forecasts can be improved somewhat beyond the performance of individual models by having a suite of multimodels and constructing a synthetic superensemble. We shall next display a geographical plot of this performance.

In Fig. 10 we show in different panels the seasonal precipitation for June, July and August 2000. Here they are expressed in the units of mm/day. The first panel (Fig. 10a) shows the observed rainfall, these can be obtained from the satellite/rain gauge mix. The other panels show the seasonal forecasts for the member models of the DEMETER models, followed by the ensemble mean of the DEMETER models, the ensemble mean of the FSU suite of models and finally the synthetic superensemble. This is generally representative of the results from this collection of models. It is clear from this example that the synthetic superensemble matches more closely the observed totals compared to any of the member models. Results of several other such fields, besides precipitation, are shown in Krishnamurti *et al.*, (2000a,b). These are not shown here, they show a similar enhancement of skill of forecasts for the synthetic superensemble compared to the member models.

6. Summary and Future Work

Monsoon forecasting is a very difficult area of science since the circulations are so intimately connected to distributions of observations over ocean and land, parameterization of cumulus convection, orography and differential heating. Large errors arise very quickly in medium range forecasts from any of these areas. The current observational network needs to be enhanced over the orographic regions where the most intense monsoon rainfall occurs. The mix of observations from satellites over ocean and from the conventional WWW need to be critically examined in the context of adaptive observation based OSSES, an area that deserves future modeling studies towards improving

the predictability of the monsoon. Here a major difficulty exists in defining a "Nature Run", since that too may have to be based on a data deficient model that does not see all possible scales adequately, such as for instance the meso scale orographic ascent in regions of steep mountains and heavy rains. These are important areas for future modeling research that can provide insights on data needs and modeling issues. We have illustrated that it is very difficult to pin down a cumulus parameterization scheme and label it as the most desirable. Most current schemes are somewhat comparable and are sensitive too initial states such that one or the other can easily have a superior performance on a given day. A way out of this difficulty seems to be a multimodel approach, Here one can construct a multi model superensemble that utilizes a suite of cumulus parameterizations in the different models and the consensus so constructed (from a superensemble), provides a weighted bias corrected product for these member models and that seems to perform the best.

With the available regional mesoscale models and a benchmark analysis, an intercomparison study (under simulated operational conditions) to assess the skill of models to predict various weather systems associated with monsoon will be quite useful for practical applicability and it will also provide further insight into the issues related to the modeling of monsoon. Such inter-comparison studies have been undertaken for other regions (Cox *et al.*, 1998). Further improvements in all of the area of physical parameterizations are needed to improve the individual models. As the models improve so will the multimodel superensemble, which always performs somewhat better than the member model.

There is increasing recognition of the important role of the MJO/ISO in its effects on the dry and wet spells of the monsoon. Thus it may be necessary to be cognizant of the phase and amplitude of the MJO/ISO and to be able to bring in these features correctly at the start of a medium range forecast. Large errors in the representation of the MJO/ISO by the model data sets can be expected to effect the medium range monsoon forecasts.

Since moisture data sets are evidently most important during the onset phase and during the transitions between the dry and the wet spells of the monsoon, it may be worthwhile to explore newer moisture profiling data sets such as those provided by the AIRS/AQUA satellites for the data assimilation. Impacts of improved moisture distributions on medium range monsoon forecasts deserve to be studied.

References

Alapaty, K., S. Raman, R.V. Madala, and U.C. Mohanty, 1994: Monsoon Rainfall Simulations with Kuo and Betts-Miller Schemes. *Meteorol. Atmos. Phys.*, **53**, 33-49.

Andre, J. C., J. P. Goutorbe, and A. Perreir, 1986: HAPEX MOBILHY: A hydrologic atmospheric experiment for the study of water budget and evaporation flux at the climatic scale. *Bull. Amer. Meteor. Soc*., **67**, 138-144.

Barker D.M., W. Huang, Y.-R. Guo, A. J. Bourgeois, and Q. N. Xiao, 2004: A Three-Dimensional Variational Data Assimilation System for MM5: Implementation and Initial Results, *Mon. Wea. Rev.*, **132**, 897–914.

Basu, S., G. R. Iyengar, and A. K. Mitra, 2002: Impact of a Nonlocal Closure Scheme in a simulation of a monsoon system over India. *Mon. Wea. Rev.*, **130**, 161-170.

Basu, S., Z.N. Begum and E.N. Rajagopal, 1998: Impact of Boundary Layer Parameterization schemes on the Prediction of the Asian summer monsoon. *Bound. -Layer Meteor.*, **86**, 469-485.

Blackadar, A. K., 1962: The vertical distribution of wind and turbulent exchanges in neutral atmosphere. *J. Geophys. Res*., **67**, 3095-3102.

Brost, R. A. and J. C. Wyngaard, 1978: A model study of the stably stratified planetary boundary layer. *J. Atmos. Sci*., **35**, 1427-1440.

Businger, J.A., J.C. Wyngard, Y. Izumi and E.F. Bradley, 1971: Flux profile relationship in the atmospheric surface layer. *J. Atmos. Sci.*, **28**, 181-189.

Chang, C. B., 1979: On the influence of solar radiation and diurnal variation of surface temperatures on African Disturbances, Rep. 79-3. Dept. of meteorology, Florida State University, Tallahassee, Fl 32306, 157 pp.

Cox, R., B.L. Bauer, and T. Smith 1998, A Mesoscale Model Intercomparison, *Bull. Amer. Met. Soc.*, **79**, 265-283.

Das S., S. V. Singh, E. N. Rajagopal, and R. Gall, 2003: Mesoscale Modeling for Mountain Weather Forecasting Over the Himalayas, *Bull. Amer. Meteorol. Soc*., **84**, 1237–1244.

Das, S., 2002: Real time mesoscale weather forecasting over Indian region using MM5 modeling system, NCMRWF Research Report No. NMRF/RR/3/2002, NCMRWF, New Delhi, India.

Dastoor, A., and T.N. Krishnamurti, 1991: The landfall and structure of a tropical cyclone: the sensitivity of model predictions to soil moisture parameterization, *Bound. Layer Meteor.*, **55**, 345-380.

Dickinson, R. E., A. Henderson-Seuers, P. J. Kennedy, and M. F. Wilson, 1986: Biosphere-atmosphere Transfer Scheme (BATS) for the NCAR Community climate Model. National Center for Atmospheric Research, Boulder Co., Tech. Note NCAR/TN–275+STR, 69pp.

Ducoudre, N., K. Laval, A. Perrier, 1993: SECHIBA, a new set of parameterizations of the hydrologic exchanges at the land/atmosphere interface within the LMD atmospheric general circulation model. *J. Climate*, **6**, 248-273.

Eitzen, Z.A., and Randall, D.A., 1999: Sensitivity of the simulated Asian summer monsoon to parameterized physical processes. *J. Geophys. Res.*, **104**, 12177-12191.

Garratt, J. R., 1993: Sensitivity of climate simulations to land surface and atmospheric boundary layer treatments – a review. *J. Climate*, **6**, 419-449.

Gates, W. L., A. Henderson-Sellers, G.J. Boer, C. K. Folland, A. Kitoh, B. J. McAvaney, F. Semazzi, N. Smith, A. J. Weaver, and Q.-C. Zeng, 1996: Climate models – evaluation. Climate Change 1995, J. T. Houghton, L. G. Meira Filho, B. A. Callander, N. Harris, A. Kattenberg and K. Maskell, Eds., 567pp.

Gill, A.E., 1980: Some simple solutions for heat-induced tropical circulation. *Quart. J. Royal Met. Soc*., **106**, 447-462.

Goswami, B.N., and P.K. Xavier, 2003: Potential predictability and extended range prediction of Indian Summer Monsoon Breaks, *Geophys. Res. Lett*., **30(18)**, 1966.

Harshvardan and T.G. Corsetti, 1984: Longwave parameterization for the UCLA/GLAS GCM. NASA Tech. Memo. 86072, Goddard Space Flight Center, Greenbelt, MD 20771, 52 pp. 51.

Henderson-Sellers, A. J. Pitman, P. K. Love, P. Irannejad, and T. H. Chen, 1995: The project for intercomparison of land surface parameterization schemes (PILPS): phases 2 and 3. *Bull. Amer. Meteor. Soc.*, **74**, 489-503.

Henderson-Sellers, Z.-L. Yang, and R. E. Dickinson, 1993: The project for intercomparison of land-surface parameterization schemes. *Bull. Amer. Meteor. Soc.*, **74**, 1335-1349.

Holtslag, A. A. M. and C. -H. Moeng, 1991: Eddy diffusivity and countergradient transport in the convective atmospheric boundary layer. *J. Atmos. Sci.*, **48**, 1690-1698.

Holtslag, A. A. M., and B. A. Boville, 1993: Local versus nonlocal boundary layer diffusion in a global climate model. *J. Climate*, **6**, 1825-1847.

Hong, S. Y, and H. L. Pan 1996: Nonlocal boundary layer vertical diffusion in a medium range forecast model. *Mon. Wea. Rev.*, **124**, 2322-2339.

Ji, Y., and A.D. Vernekar, 1997: Simulations of the Asian summer monsoons of 1987 and 1988 with a regional model nested in a global GCM, *J. Climate*, **10**, 1965-1979.

Kanamitsu, M., 1975: On numerical prediction over a global tropical belt. Report No. 75-1, Dept. of Meteorology, Florida State University, Tallahassee, Florida 32306, pp. 1-282.

Kanamitsu, M., K.Tada, K. Kuda, N. Sato, and S. Isa, 1983: Description of the JMA operational spectral model. *J. Meteor. Soc. Japan*, **61**, 812-828.

Kanamitsu, M., 1989: Description of the NMC global data assimilation and forecast system. *Weather and Forecasting*, **4**, 335-342.

Kanamitsu, M., and H.-M.H, Juang, 1994: Multi month simulations of Indian Monsoon by the NMC nested regional spectral model. *Preprints , 10th conference on NWP*, Portland, OR, AMS, 351-352.

Kishtawal, C.M., and T.N. Krishnamurti, 2001: Diurnal variation of summer rainfall over Taiwan and its detection using TRMM observations. *J. Appl. Meteorol.*, **40**, 331-344.

Krishnamurti, T.N., 1969: An experiment in numerical prediction in equatorial latitudes. *Quart. J. Royal Meteorol. Soc.*, **95**, 594-620.

Krishnamurti, T.N., and D. Subrahmanyam, 1982: The 30-50 day mode at 850 mb during MONEX. *J. Atmos. Sci*., **39**, 2088-2095.

Krishnamurti, T.N., S. Low-Nam, and R. Pasch, 1983: Cumulus parameterization and Rainfall Rates – II. *Mon. Wea. Rev.*, 111, 815-828.

Krishnamurti, T.N., 1987a: NWP in low latitudes. *Adv. in Geophysics*, **28**, 283-333.

Krishnamurti, T.N., S. Low-Nam, A. Kumar, J. Sheng, and M. Sugi, 1987b: Numerical weather prediction of monsoons. *Monsoon Meteorology*, Eds. C.-P. Chang and T.N. Krishnamurti, Oxford Monographs on Geology and Geophysics, Oxford University Press, 501-544.

Krishnamurti, T.N., H.S. Bedi, and W. Han, 1998a: Organization of convection and monsoon forecasts. *Meteorol. Atmos. Phys.*, **67,** 117-134.

Krishnamurti, T.N., H.S. Bedi and V.M. Hardiker, 1998b: *An introduction to global spectral modeling*. Oxford University Press, 253pp.

Krishnamurti, T.N., 1990a: Monsoon prediction at different resolutions with a global spectral model. *Mausam*, **41**, 234-240.

Krishnamurti, T.N., A. Kumar, K.S. Yap, A.P. Dastoor, N. Davidson, and J. Sheng, 1990b: Performance of a high-resolution mesoscale tropical prediction model, *Advances in Geophysics*, **32**, Academic Press Inc., 133-286.

Krishnamurti, T.N., M. Subrahmaniam, D.K. Oosterhof, and G. Daughenbaugh, 1990c: Predictability of low frequency modes. *Meteorol. Atmos. Phys*., **44**, 63-83.

Krishnamurti, T. N., J. Xue, H. S. Bedi, K. Ingles, and D. Oosterhof, 1991: Physical initialization for numerical weather prediction over the tropics. *Tellus*, **43AB**, 53-81.

Krishnamuti, T.N., M.C. Sinha, R. Krishnamurti, D. Oosterhof, and J. Comeaux, 1992: Angular momentum, length of day and monsoonal low frequency mode. *J. Met. Soc. Japan*, **70**, 131-166.

Krishnamurti, T. N., C. M. Kishtawal, T. LaRow, D. Bachiochi, Z. Zhang, C. E Williford, S. Gadgil, and S. Surendran, 1999: Improved weather and seasonal climate forecasts from multimodel superensemble. *Science*, **285**, 1548-1550.

Krishnamurti, T. N., C.M. Kishtawal, Z. Zhang, T. LaRow, D. Bachiochi, C. E. Williford, S. Gadgil, and S. Surendran, 2000a: Multimodel ensemble forecasts for weather and seasonal climate. *J. Climate*, **13**, 4196-4216.

Krishnamurti, T. N., C. M. Kishtawal, D. W. Shin, and C. E. Williford, 2000b: Improving Tropical Precipitation Forecasts from a Multianalysis Superensemble. *J. Climate*, **13**, 4217-4227.

Krishnamurti, T. N., S. Surendran, D. W. Shin, R. J. Correa-Torres, T. S. V. Vijaya Kumar, C. E. Williford, C. Kummerow, R. F. Adler, J. Simpson, R. Kakar, W. S. Olson, and F. J. Turk, 2001: Real-Time Multianalysis-Multimodel Superensemble Forecasts of Precipitation Using TRMM and SSM/I Products. *Mon. Wea. Rev*., **129**, 2861-2883.

Krishnamurti, T.N., Lydia Stefanova, Arun Chakraborty, T.S.V. Vijaya Kumar, Steve Cocke, David Bachiochi, and Brian Mackey, 2002: Seasonal Forecasts of precipitation anomalies for North American and Asian Monsoons. *J. Met. Soc. Japan*, **80**, 1415-1426.

Krishnamurti, T. N. and J. Sanjay, 2003: A New Approach to the cumulus parameterization issue. Accepted for publication, *Tellus A*.

Krishnamurti, T. N., A. K. Mitra, W. T. Yun, T. S. V. Vijaya Kumar and William K. Dewar, 2004: Seasonal Climate Forecasts of the Asian Monsoon Using Multiple Coupled Models. Submitted to *J. Climate*.

Krishnan R., and Kasture S.V., 1996: Modulation of low frequency intraseasonal oscillation of the northern summer monsoon by El Nino and Southern Oscillation (ENSO). Meteorol. and Atmos. Phys., **30**, 2237-257.

Kuo, H.L., 1965: On formation and intensification of tropical cyclones through latent heat release by cumulus convection. *J. Atmos. Sci*., **22**, 40-63.

Lacis, A.A. and J.E. Hansen, 1974: A parameterization for absorption of solar radiation in the Earth's atmosphere, *J. Atmos. Sci*., **31**, 118-133.

Louis, J.F., 1979: A parametric model of vertical eddy fluxes in the atmosphere. *Boundary Layer Meteorology*, **17**, 187-202.

Madala, R.V., S. W. Chang, U. C. Mohanty, S. C. Madan, R. K. Paliwal, V. B. Sarin, T. Holt, and S. Raman, 1987: Description of Naval Research Laboratory limited area dynamical weather prediction model. NRL Tech. Rep. 5992, Washington, DC, 131 pp. [Available from Naval Research Laboratory, Washington, DC 20375.]

Mahfouf, J.-F., A.O. Manzi, J. Noilhan, H. Giordani, and M. Deque, 1995: The land surface scheme ISBA within the Meteo-France climate model ARPEGE. Part I: Implementation and preliminary results. *J. Climate*, **8**, 2039-2057.

Mahfouf, J.-F., C. Ciret, A. Ducharne, P. Iranejad, J. Noilhan, Y. Shao, P. Thornton, Y. Xue, Z.-L. Yang, 1996: Analysis of transpiration results from the RICE and PILPS workshop. *Glob. and Planet. Change*, 13, 73-88.

Manabe, S., 1969: Climate and the ocean circulation 1. the atmospheric circulation and the hydrology of the earth's surface. *Mon. Wea. Rev.*, **97**, 739-774.

O'Brien, J.J., 1970: A note on the vertical structure of the eddy exchange coefficient in the planetary boundary layer. *J. Atmos. Sci.*, 27, 1213-1215.

Palmer, T.N., and collaborators, 2004: Development of a European Multi-Model Ensemble System for Seasonal to Inter-Annual Prediction (DEMETER), *Bull. Amer. Met. Soc*., **85**, 853 – 872.

Prandtl, L., 1932: Meteorologische Anwendungen der Stromungslchre, *Beitr. Phys. Atmos*., **19**,188-202.

Rajagopal, E.N., and G.R. Iyengar, 2002: Implementation of Mesoscale Eta model at NCMRWF, NCMRWF Research Report No. NMRF/RR/4/2002, NCMRWF, India, 28p.

Rajendran, K.R., R.S. Nanjundiah and J. Srinivasan, 2002: Comparison of seasonal and intraseasonal variation of tropical climate in NCAR CCM2 GCM with two different cumulus schemes. *Meteorol. Atmos. Phys*., **79**, 3921-3926.

Raman, S., U.C. Mohanty, N.C Reddy, K. Alapaty and R.V. Madala, 1998: Numerical Simulation of the Sensitivity of Summer Monsoon Circulation and Rainfall over India to Land Surface Processes. *Pure Applied Geophysics*, **152**,781-809.

Rao, Y.V.R., K. Prasad and Sant Prasad, 2001: A case study of the impact of INSAT derived humidity profiles on precipitation forecast by limited area model, *Mausam,* **52**,647-654.

Roy Bhowmik, S.K., and Prasad K, 2001: Some characteristics of limited area model precipitation forecast of Indian monsoon and evaluation of associated flow features, *Meteorol. Atmos. Phys.*, **76**, 223-236.

Roy Bhowmik, S.K, 2003: Monsoon rainfall prediction with a nested grid mesoscale limited area model over Indian Region. *Proc. India Acad. Sc*., **112**, 499-520

Sanjay, J., P. Mukhopadhyay, and S. S. Singh, 2002: Impact Of Nonlocal Boundary Layer Diffusion Scheme On Forecasts Over Indian Region. *Meteor. Atmos. Phys*., **80**, 207-216.

Sellers, P. J., Y. Mintz, Y.C. Sud, and A. Dalcher, 1986: A simple biosphere model (SiB) for use within general circulation models. *J. Atm. Sci.*, **43**, 505-531.

Sellers, P. J., F. Hall, H. Margolis, B. Kelly, D. Baldocchi, G. den Hartog, J. Cihlar, M. G. Ryan, B. Goodison, P. Crill, K. J. Ranson, D. Lettenmaier, and D. Wickland, 1995: The Boreal Ecosystem-Atmosphere Study (BOREAS): an overview and early results from the 1994 field year. *Bull. Amer. Meteor. Soc.* **76**, 1549-1577.

Slingo, J., M. Blackburn, A. Betts, R. Brugge, K. Hodges, B. Hoskins, M. Miller, L. Steenmanclark, and J. Thuburn, 1994: Mean climate and transience in the tropics of the UGAMP GCM - sensitivity to convective parameterization. *Quart. J. Royal Met. Soc.*, **120**, 881-922.

Stull, R. B., 1988: An Introduction to Boundary Layer Meteorology. Kluwer Academic Publishers, Dordrecht. 666pp.

Tiedtke, M., 1984: The sensitivity of the time-mean large-scale flow to cumulus convection in the ECMWF model. Workshop on convection in large-scale numerical models. ECMWF, 28 Nov. - 1 Dec. 1983, 297-316.

Treadon, R.E., 1996: Physical initialization in the NMC global data assimilation system. *Meteorol. Atmos. Phys.*, **60**, 57-86.

Troen and Mahrt 1986: A simple model of the atmospheric boundary layer; Sensitivity to surface evaporation. *Bound. –Layer Meteor.*, **37**, 129-148.

Vaidya, S. S., P. Mukhopadhyay, D. K. Trivedi, J. Sanjay and S. S. Singh, 2004: Prediction of tropical systems over Indian region using mesoscale model. *Meteorol. Atmos. Phys*., **86**, 63-72.

Wallace, J.M., S. Tibaldi and A.J. Simmons, 1983: Reduction of systematic forecast errors in the ECMWF model through the introduction of envelope orography. *Quart. J. Roy. Met. Soc*., 109, 683-718.

Wu, Y., S. Raman, and U.C. Mohanty, 1999: Numerical investigation of Somali jet interaction with the western Ghat mountains, *Pure and Applied Geophysics*, **154**, 365-396.

Xie, P., and P.A. Arkin, 1997: Global Precipitation: A 17 year monthly analysis based on observations, satellite estimates & numerical model outputs, *Bull. Amer. Met. Soc*., **78**, 2539 2558.

Xue, Y., P. J. Sellers, J. L. Kinter, and J. Shukla, 1991: A simplified biosphere model for global climate studies. *J. Climate*, **4**, 345-364

Yanai, M., S. Esbensen and J.H. Chu, 1973: Determination of bulk properties of tropical cloud clusters from large-scale heat and moisture budgets. *J. Atmos. Sci.*, **30**, 611-627.

Yun, W.T., L. Stefanova, A. K. Mitra, T.S.V. Vijaya Kumar, W. Dewar and T. N. Krishnamurti, 2004: Multimodel synthetic superensemble algorithm for seasonal climate prediction using DEMETER forecasts, *Tellus* (Accepted for publication).

Zhang, G.J., 1994: Effects of cumulus convection on the simulated monsoon circulation in a general circulation model. *Mon. Wea. Rev.*, **122**, 2022-2038.

Zhang, Z. and T.N. Krishnamurti, 1996: A generalization of Gill's heat-induced tropical circulation. *J. Atmos. Sci.*, **53**, 1045-1052.

Zhao, Qingyun, 1997: A Prognostic Cloud Scheme for Operational NWP Models. *Mon. Wea. Rev.,* 125, 1931-1953.

Appendix I: Outline of the FSU Global Spectral Model

The global model used in this study is identical to that used in Krishnamurti *et al.* (1998). The following is an outline of the global model:

(a) Independent variables: (x, y, σ, t).

(b) Dependent variables: vorticity, divergence, surface pressure, vertical velocity, temperature and humidity.

(c) Horizontal resolution: Triangular truncation at different wave numbers.

(d) Vertical resolution: 15 layers between roughly 10 and 1000 mb.

(e) Semi-implicit time differencing scheme.

(f) Envelope orography (Wallace *et al.*, 1983).

(g) Centered differences in the vertical for all variables except humidity, which is handled by an upstream differencing scheme.

(h) Fourth order horizontal diffusion (Kanamitsu *et al.*, 1983).

(i) Kuo-type cumulus parameterization (Krishnamurti *et al.*, 1983).

(j) Shallow convection (Tiedtke, 1984).

(k) Dry convective adjustment.

(l) Large-scale condensation (Kanamitsu, 1975).

(m) Surface fluxes via similarity theory (Businger *et al.*, 1971).

(n) Vertical distribution of fluxes utilizing diffusive formulation where the exchange coefficients are functions of the Richardson number (Louis, 1979).

(o) Long and shortwave radiative fluxes based on a band model (Harshvardan and Corsetti, 1984; Lacis and Hansen, 1974).

(p) Diurnal cycle.

(q) Parameterization of low, middle and high clouds based on threshold relative humidity for radiative transfer calculations

(r) Surface energy balance coupled to the similarity theory (Krishnamurti *et al.*, 1991)

(s) Nonlinear normal mode initialization - 5 vertical modes (Kitade, 1983).

(t) Physical initialization (Krishnamurti *et al.*, 1991).

Appendix II: Definitions of statistical parameters (skill metrics)

RMS Error = $\left[\frac{1}{N}\sum_{n=1}^{N}(f_n - o_n)^2\right]^{1/2}$

Systematic Error (Bias) = $\frac{1}{N}\sum_{n=1}^{N}(f_n - o_n)$

Anomaly Correlation = $\frac{\sum_{n=1}^{N}[(f_n - c_n)(o_n - c_n)]}{\left[\sum_{n=1}^{N}(f_n - c_n)^2 \sum_{n=1}^{N}(o_n - c_n)^2\right]^{1/2}}$ (AC > 0.6 for useful forecast skill)

Correlation Coefficient = $\frac{\sum_{n=1}^{N}[(f_n - \bar{f})(o_n - \bar{o})]}{\left[\sum_{n=1}^{N}(f_n - \bar{f})^2 \sum_{n=1}^{N}(o_n - \bar{o})^2\right]^{1/2}}$ ($-1 \le c \le 1$)

Equitable Threat Score = $\frac{H - \left(F \times \frac{O}{N}\right)}{F + O - H - \left(F \times \frac{O}{N}\right)}$ ($0 \le ETS \le 1$)

Bias = $\frac{N_f}{N_o}$

In these expressions:

N = number of grid points
fn = forecast value at grid point n
on = observed value at grid point n
cn = climatological (mean) value at grid point n
$\bar{f}$ = area mean of the forecasted values
$\bar{o}$ = area mean of the observed values
F = area where event is forecasted
O = area where event is observed
H = hit area, or overlap of areas F and O
Nf = number of grid points where event is forecasted
No = number of grid points where event is observed

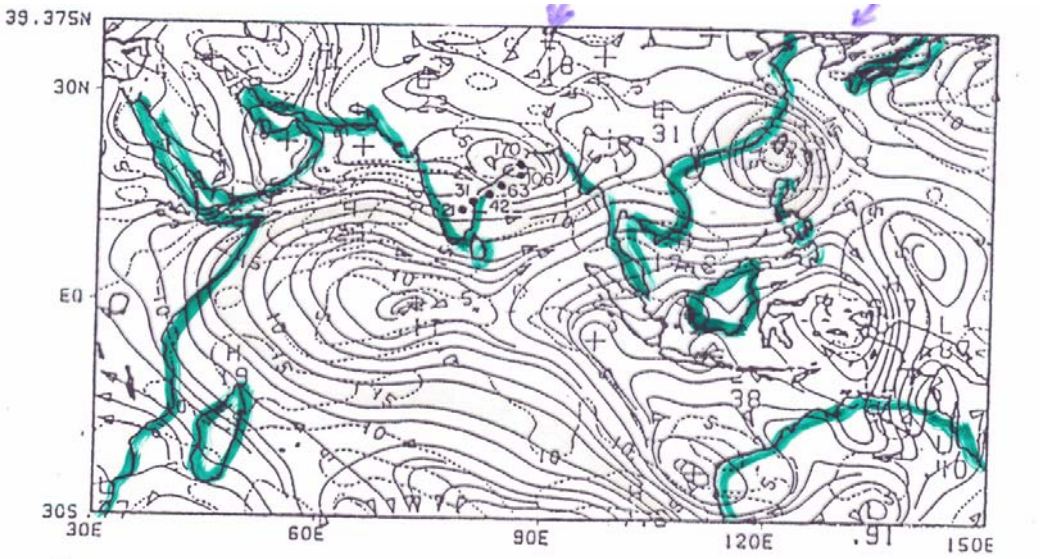

Figure 1: 120-hr forecasts of streamlines at 850 hPa using global model at varying horizontal resolutions T21, T31, T42, T63 and T106 and T170. The black dots along the east coast of India denote the positions of the monsoon depression. The flow field shown via streamlines is the observed field on day 5.

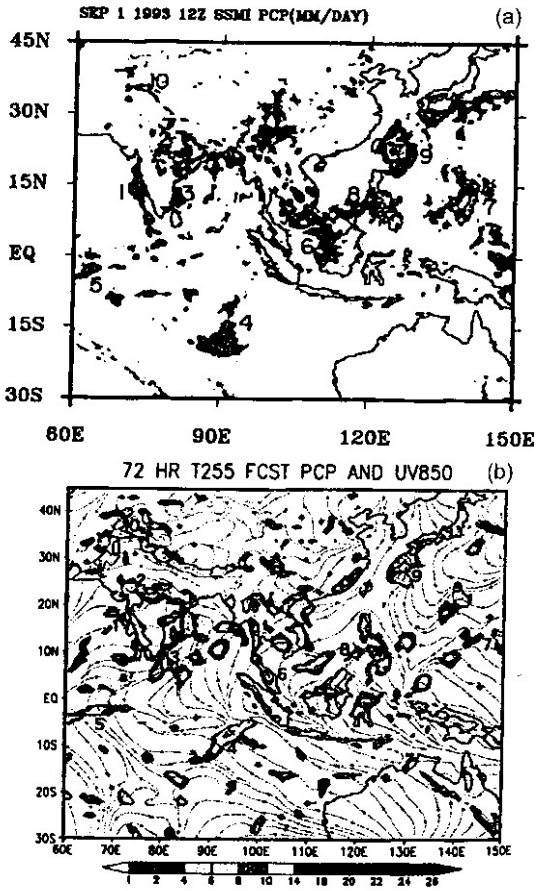

Figure 2: (a) Observed 24 hour rainfall valid 12 UTC of September 1, 1995 (mm day-1); (b) 72-hr forecast of 850 hPa flow field with superimposed accumulated rainfall (mm day-1) using global model at T255 resolution.

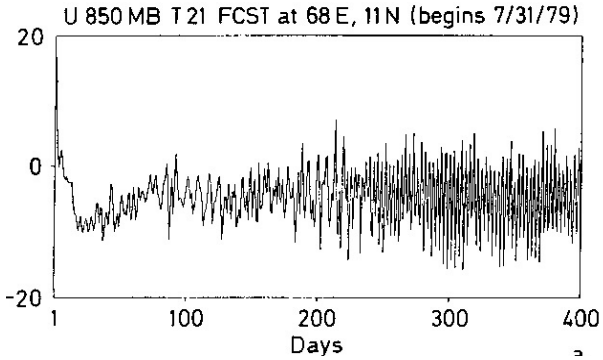

Figure 3: Time history of the zonal wind at 850 hPa along 68oE from the anomaly experiment (ms-1) using FSU global model at T21 resolution.

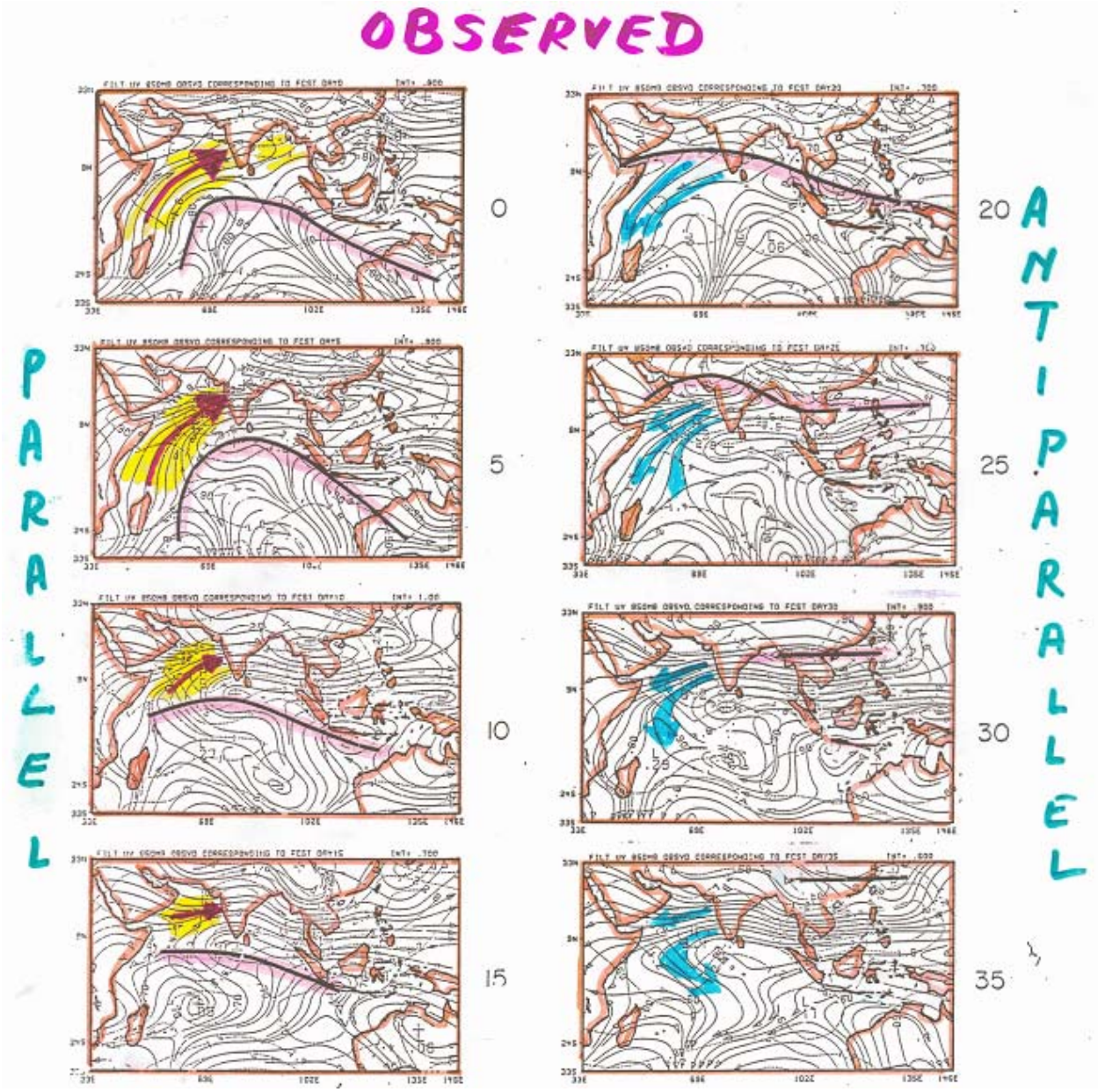

Figure 4: A sequence of 850 hPa observed flow fields (time filtered on the scale of 30 to 50 days) for the experiment on dry spell over India. Streamlines (solid lines) and isotachs (ms-1) are shown here.

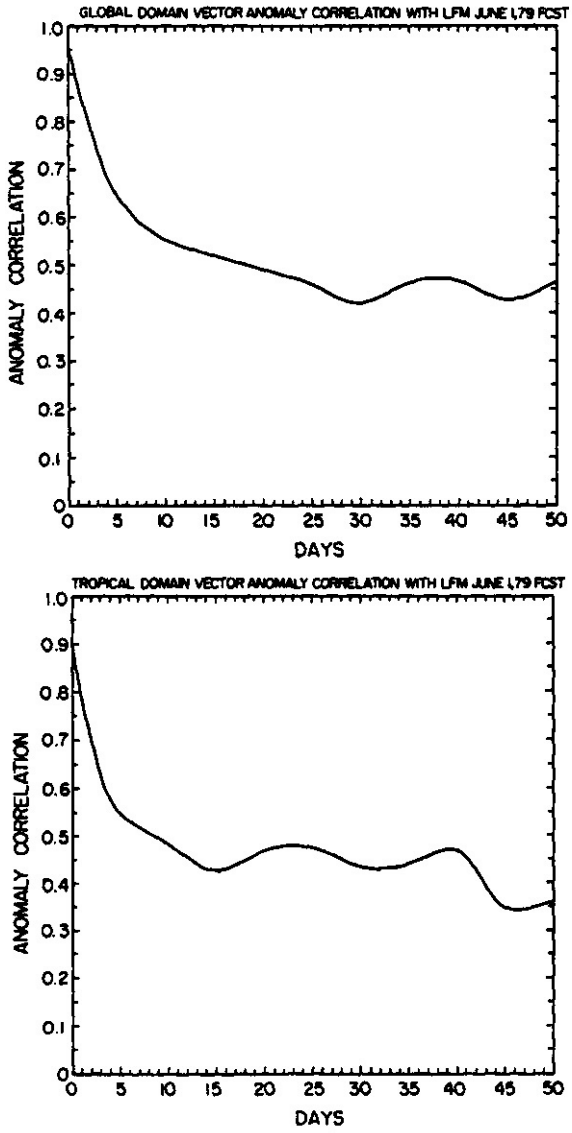

Figure 5: Anomaly Correlations of forecasts as a function of days of forecasts for (a) globe and (b) tropics.

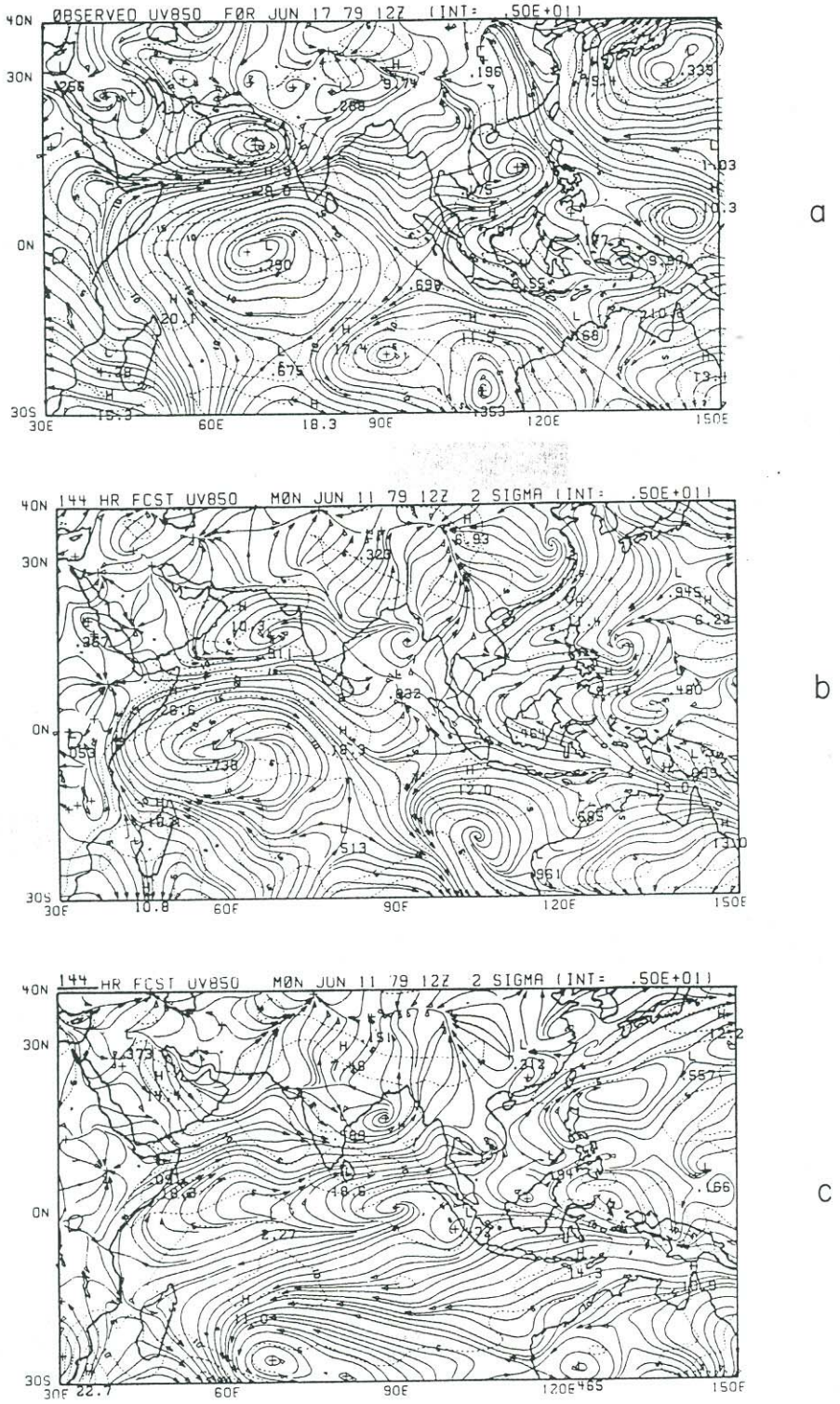

Figure 6: The 850 hPa flow field for June 17, 1979 (12 GMT). (a) Observed flows (b) A six-day forecast from a modification of Kuo's scheme (c) A corresponding six-day forecast made from the classical scheme of Kuo.

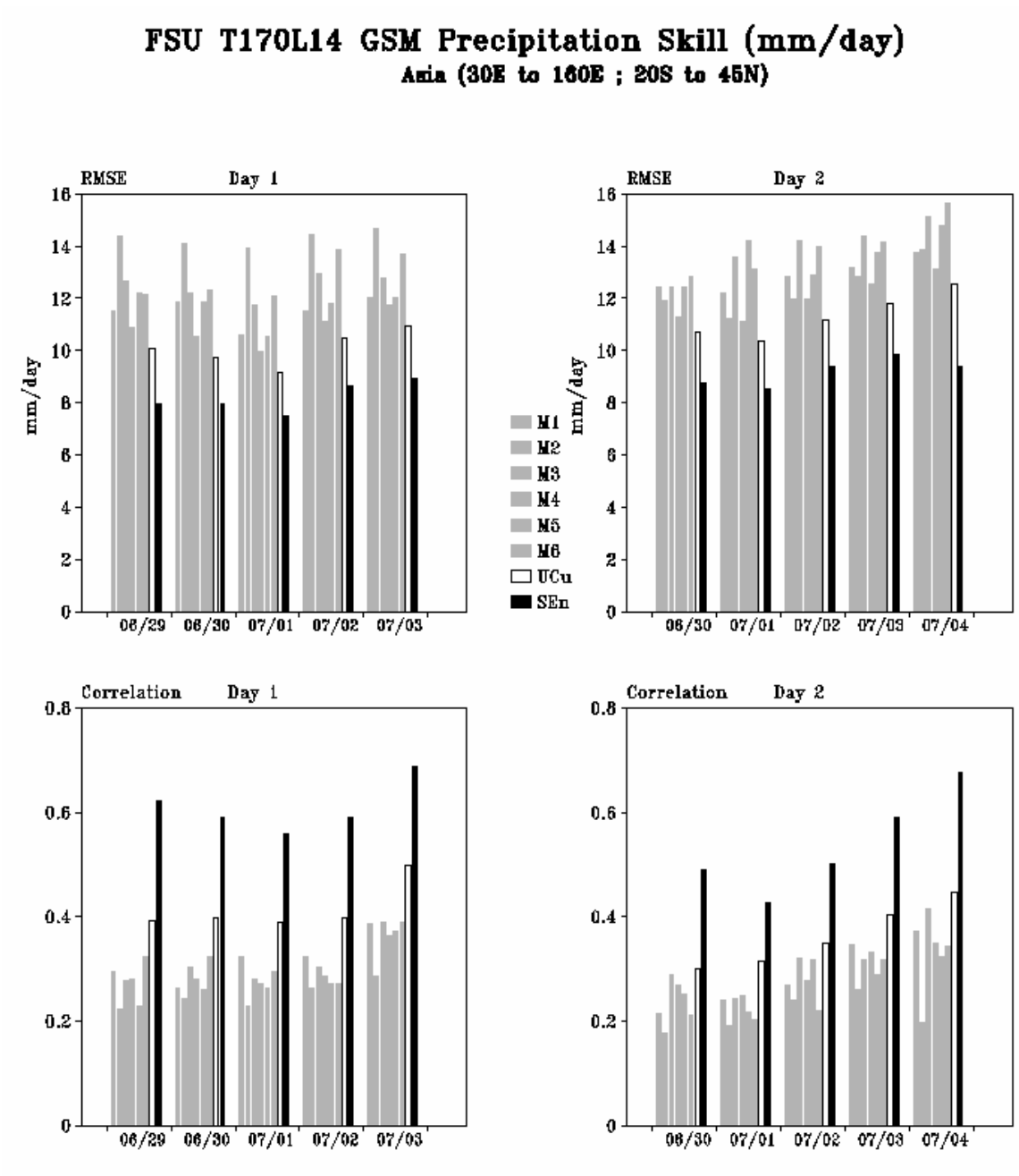

Figure 7: RMS Error Skill (mm/day) and anomaly correlation of precipitation forecasts at day 1 (left panels) and day 2 (right panels) of forecasts from FSU Global Spectral Model at T170 resolution, using different cumulus convection parameterization schemes (M1 through M6), Unified Convection Scheme (UCu) and the Superensemble (SEn).

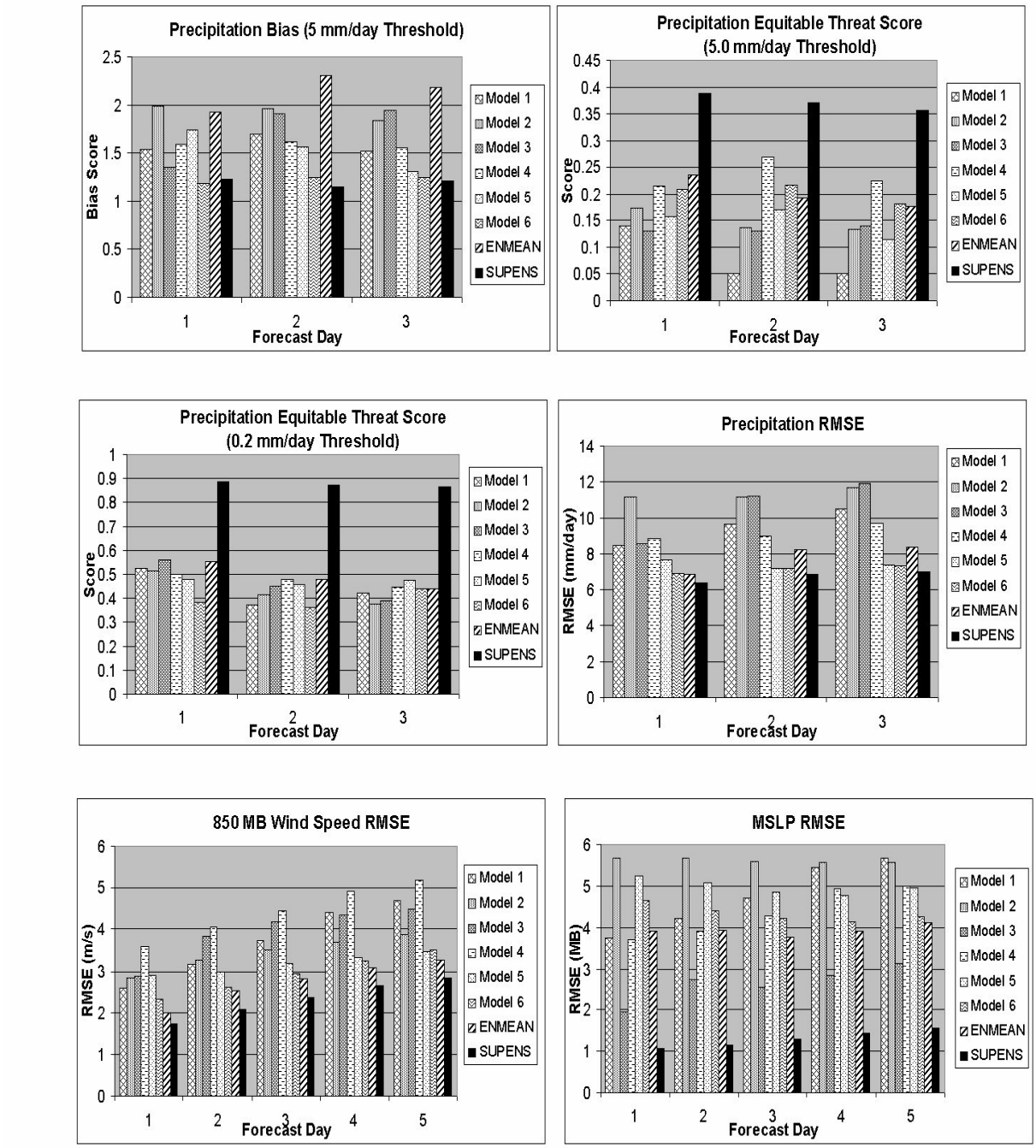

Figure 8: Various skill scores for the Asian Summer Monsoon Region (10ºS to 35ºN and 50ºE to 110ºE) from different member models, their ensemble mean and the superensemble. (a) Precipitation Bias Score at 5 mm/day threshold (b) Precipitation Equitable Threat Score at 5 mm/day threshold (c) Precipitation Equitable Threat Score at 0.2 mm/day threshold (d) Precipitation RMS Error (mm/day) (e) 850 hPa wind RMS error (ms-1) and (f) Mean Sea Level Pressure RMS Error (hPa).

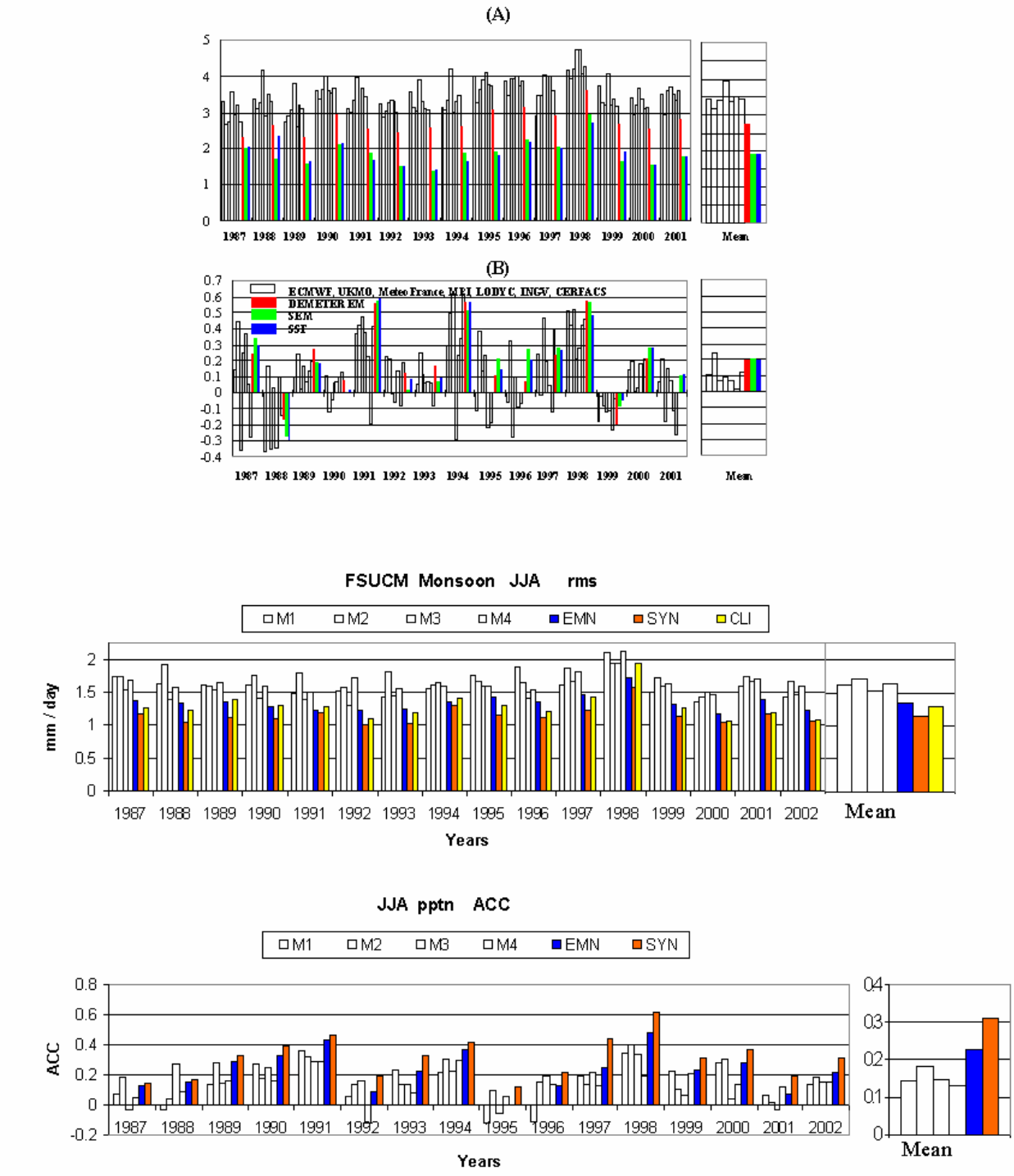

Figure 9: (a) RMS errors and anomaly correlation of precipitation forecasts for different years for 7 DEMETER models, ensemble mean of the 7 DEMETER models, synthetic ensemble mean, and for the synthetic super ensemble; Domain is for Asian Summer Monsoon (50ºE to 110ºE and from 10ºS to 35ºN). Units for rms mm/day. (b) Same as Fig. 9a, but for the suite of 4 FSU coupled models.

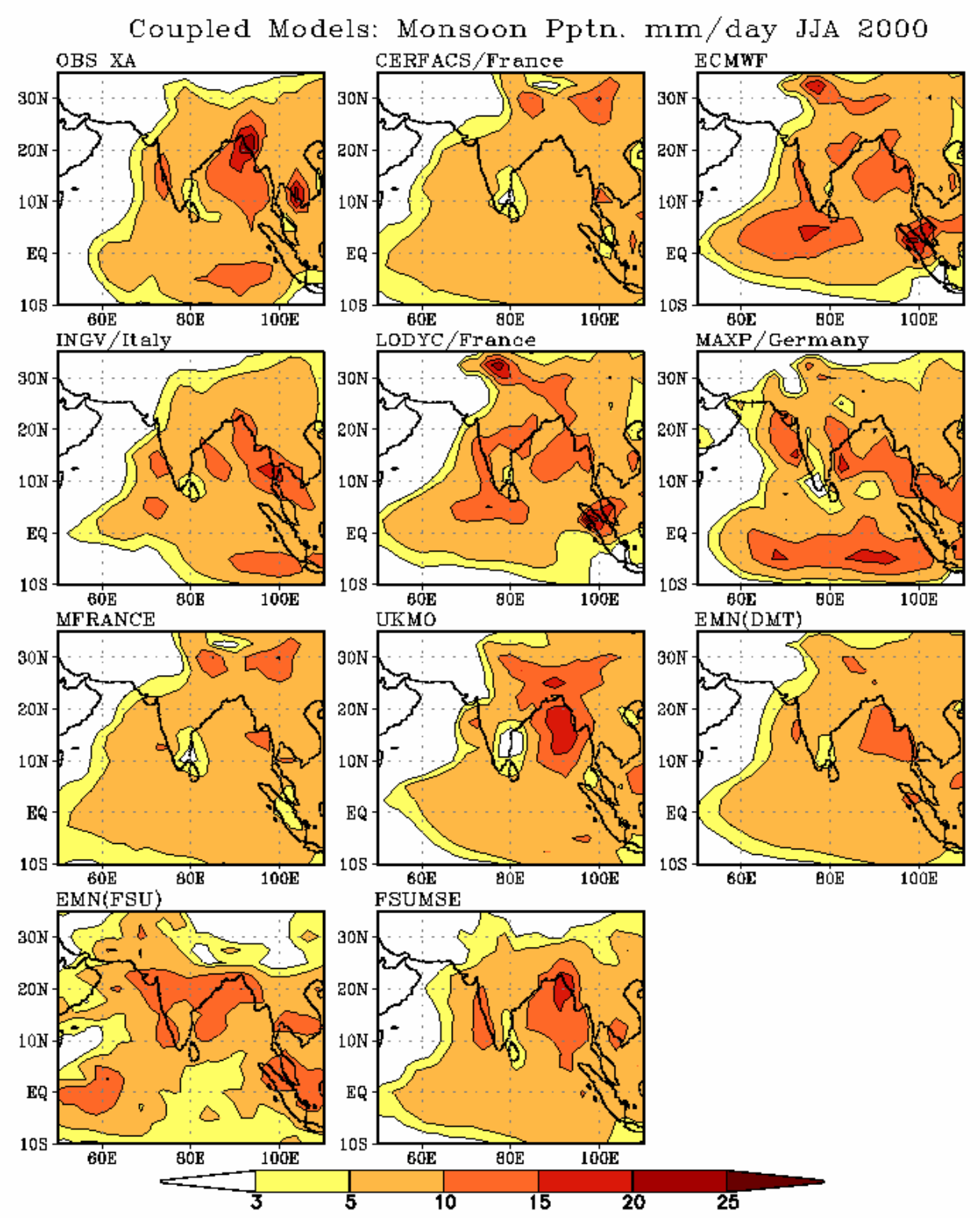

Figure 10: An example of seasonal forecast of precipitation (mm/day) for a relatively wet monsoon year 2000 is shown. The observed estimates from Xie and Arkin (1997), from the member models of DEMETER and those from the ensemble mean of the four FSU models and those from the FSU synthetic superensemble are shown.

Table 1. Features of different cumulus parameterization schemes

Sr. No:	Cumulus Scheme	Environmental Trigger *(Modulation of convection by large-scale)*	Cloud Model *(Treatment of cloud thermodynamic properties)*	Final State of Atmosphere *(Quantitative effects of convection on environment)*
1.	FSU Modified Kuo	Integrated vertical advection of moisture.	Moist adiabatic lapse rate. No downdrafts.	Tends towards local moist adiabat
2.	GSFC Relaxed Arakawa-Schubert	Rate of destabilization by advective changes.	Entraining plume model. Invokes single members of a cloud ensemble one after the other. Normalized cloud updraft mass flux linear function of height. No downdrafts.	Relaxes to steady state clouds in prescribed time.
3.	NRL Relaxed Arakawa-Schubert	Rate of destabilization by advective changes.	Includes evaporation of falling rain. With downdrafts.	Relaxes to steady state clouds in prescribed time.
4.	NCEP Simplified Arakawa-Schubert	Rate of change of stability. Upward vertical velocity at cloud base.	Only the deepest cloud considered. Moisture detrainment from convective clouds. Warming from environmental subsidence. Downdrafts and evaporation of falling rain included.	Adjusts toward an equilibrium cloud work function within a specified time.
5.	NCAR Zhang and McFarlene	Plumes of updraft ensemble need to be sufficiently buoyant to penetrate through locally conditional unstable lower troposphere.	Ensemble of entraining updrafts with associated saturated downdrafts.	Removes CAPE at an exponential rate with a specified time. Neutrally buoyant for undiluted reversible ascent of a parcel.
6.	NRL Emanuel	First level of neutral buoyancy for the undiluted, reversible ascent of near surface air is at a higher altitude than level of cloud base.	Sub cloud scale drafts using buoyancy-sorting technique. Determines mass flux prognostically. Stochastic coalescence and Bergeron-Findeisen mechanism. Cloud water in excess of a threshold amount converted to precipitation. Saturated and unsaturated downdrafts.	Adjusts to a local quasi-equilibrium situation, does not depend on the relaxation of cloud work function.

Table 2: Details of the seven DEMETER Coupled Models

	CERFACS France	**ECMWF**	**INGV** Italy	**LODYC** France
Atmos Model	**ARPEGE**	**IFS**	**ECHAM-4**	**IFS**
Resolution	**T63 31 Levs**	**T95 40 Levs**	**T42 19 Levs**	**T95 40 Levs**
Atmos. IC	**ERA-40**	**ERA-40**	**Coupled AMIP-type**	**ERA-40**
Ocean Model	**OPA 8.2**	**HOPE-E**	**OPA 8.1**	**OPA 8.2**
Resolution	**2° x 2° 31 Levs**	**1.4°x0.3°–1.4° 29 levs**	**2°x 0.5°–1.5° 31 levs**	**2°x2° 31 Levs**
Ocean IC	**Forced by ERA40**	**Forced by ERA40**	**Forced by ERA40**	**Forced by ERA40**

	M-France	**UKMO**	**MPI** Germany
Atmos Model	**ARPEGE**	**ARPEGE**	**ECHAM-5**
Resolution	**T63 31 Levs**	**2.5°x 3.75 ° 19 Levs**	**T42 19 Levs**
Atmos. IC	**ERA-40**	**ERA-40**	**Coupled Run Relax to Obs sst**
Ocean Model	**OPA 8.0**	**GloSea OGCM HadCM3 based**	**MPI-OMI**
Resolution	**182 x 152 GP 31 Levs**	**1.25°x0.3°-1.25° 40 Levs**	**2.5° x 0.5°–2.5° 23 Levs**
Ocean IC	**Forced by ERA40**	**Forced by ERA40**	**Coupled Run Relax to Obs sst**

(Further Details of the above coupled models can be found in Palmer *et al.*, 2004.)

Table 3: Details of the versions of the FSU Coupled Models

	KOR	**KNR**	**AOR**	**ANR**
Atmos Model	**FSUGSM**	**FSUGSM**	**FSUGSM**	**FSUGSM**
Resolution	**T63 / 14 Levs**	**T63 /14 Levs**	**T63 /14 Levs**	**T63 /14 Levs**
Atmos. IC	**ECMWF with Phy. Init**	**ECMWF with Phy. Init**	**ECMWF with Phy. Init**	**ECMWF with Phy. Init**
Atmos. Physics	**Kuo Radiation Old (Emissivity / Absorbtivity Based)**	**Kuo Radiation New (Band Model)**	**SAS Radiation Old (Emissivity / Absorbtivity Based)**	**SAS Radiation New (Band Model)**
Ocean Model	**HOPE Global**	**HOPE Global**	**HOPE Global**	**HOPE Global**
Resolution	**5° x 0.5°- 5 ° 17 Levs**	**5° x 0.5°- 5° 17 Levs**	**5° x 0.5°- 5° 17 Levs**	**5O x 0.5O- 5 O 17 Levs**
Ocean IC	**Coupled Assimilation Relax Obs SST**	**Coupled Assimilation Relax Obs SST**	**Coupled Assimilation Relax Obs SST**	**Coupled Assimilation Relax Obs SST**